Geochimica et Cosmochimica Acta 352 (2023) 36–50

Contents lists available at ScienceDirect

Geochimica et Cosmochimica Acta

journal homepage: www.elsevier.com/locate/gca

Preservation of stable isotope signatures of amino acids in diagenetically altered Middle to Late Holocene archaeological mollusc shells

N.L. Vokhshoori [a,b,*], T.C. Rick [a], T.J. Braje [c], M.D. McCarthy [b]

[a] Smithsonian Institution, National Museum of Natural History, Dept. of Anthropology, 10th St. & Constitution Ave. NW, Washington, DC 20560, USA
[b] University of California Santa Cruz, Dept. of Ocean Science, 1156 High Street, Santa Cruz, CA 95060, USA
[c] San Diego State University, Dept. of Anthropology, 5500 Campanile Drive, San Diego, CA 92182, USA

ARTICLE INFO

Associate editor: Ruth Blake

Keywords:
Diagenesis
Compound-specific isotope analysis
Amino acids
Archaeological mollusc shell
Shell bound organic matter

ABSTRACT

Stable isotope proxies measured in the proteinaceous fraction of archaeological mollusc shell represents an increasingly important archive for reconstructing past ecological and biogeochemical conditions of nearshore environments. A major issue, however, is understanding the impact of diagenetic alteration in sub-fossil shell isotope values. "Bulk" stable isotope values of nitrogen ($\delta^{15}N$), and especially carbon ($\delta^{13}C$) often shift strongly with increasing C/N ratios in degraded shell, resulting in unreliable data. Here, we examine preservation of an entirely new set of shell paleo-proxies, compound-specific isotopes of amino acids (CSI-AA). We examine carbon ($\delta^{13}C_{AA}$) and nitrogen ($\delta^{15}N_{AA}$) patterns and values from the organic fraction of California mussel (*Mytilus californianus*) shells from the California Channel Islands. Archaeological shell samples ranging in age from ca. 6,100 to 250 cal BP exhibiting a wide range of degradation states were collected from varied depositional environments (e.g., exposed coastal bluff, buried strata, etc.), and were directly compared to modern shells of the same species and region.

Our results indicate organic matter C/N ratios as the best bulk diagnostic indicator of the relative degradation state of shell organic fraction, including changes at the molecular level. Modern shell organic C/N ratios ranged from 2.8 to 3.5, while those in archaeological shell were substantially elevated (3.4–9.5), exhibiting strong and significant negative correlations with bulk $\delta^{13}C$ values, weight %C, and weight %N, and a significant but weaker correlation with δ^{15} N values. An additional "cleaning" step using weak NaOH helped to remove possible exogenous contaminants and improved bulk values of some samples. However, relative molar AA abundances revealed that some AAs, especially the two most abundant, Glycine and Alanine, progressively decreased with increasing C/N ratio. The loss of these amino acids permanently alters bulk isotope values regardless of removal of contaminants. Modeling the bulk isotope change expected due to amino acid molar composition showed major and predictable shifts in bulk $\delta^{13}C$ values from selected AA loss, and similarly large but far more variable impacts from exogenous contaminants.

In contrast to bulk data, key CSI-AA values and patterns remained almost entirely unaltered, even in the most degraded shell samples, closely matching expected biosynthetic isotope patterns in modern mussel shell. AA isotope proxies for "baseline" (δ^{15}N-Phenylalanine and average δ^{13}C-Essential AAs) and planktonic trophic structure (δ^{15}N-Glutamic Acid and δ^{15}N-Phenylalanine) were not statistically altered with degradation in any sample. Overall, we conclude that while bulk isotopes, particularly $\delta^{13}C$, are very likely to be unreliable in archaeological or subfossil shell with C/N ratios higher than ~4.0, CSI-AA proxies can still be used to reconstruct past climatic and ecological conditions of the nearshore marine environment.

1. Introduction

Mollusc shells are among the most abundant skeletal hard parts preserved in coastal archaeological sites, representing one of the best archives for reconstructing past coastal palaeoecological and palaeoceanographic conditions (Andrus, 2011; Prendergast and Stevens,

* Corresponding author at: Smithsonian Institution, National Museum of Natural Hisotry, Dept. of Anthropology, 10th St. & Constitution Ave. NW, Washington DC 20560, USA.
E-mail address: natasha.vokhshoori@gmail.com (N.L. Vokhshoori).

https://doi.org/10.1016/j.gca.2023.05.005
Received 8 July 2022; Accepted 9 May 2023
Available online 16 May 2023

2014; Leng and Lewis, 2016). In the face of a rapidly changing climate, habitat loss, and pollution, coastal marine ecosystems display widely different responses to climatic perturbations. Impacts related to major upwelling margins can be particularly difficult to predict from basin scale patterns alone; one recent example was the 2014–2016 marine heatwave (McClatchie et al., 2016), which resulted in massive ecological damage in the Pacific Northwest, while coastal communities in southern California were far less impacted (Sakuma et al., 2016). The need for bioarchives that can reconstruct highly detailed, coastal margin oceanographic conditions will therefore be critically important for understanding how different coastal communities might have responded to climatic perturbations in the historical and geologic past.

In marine shell, sea surface temperature reconstructions from oxygen isotopes ($\delta^{18}O$) are commonly performed on the carbonate fraction. However, a small but significant percentage of shell is also composed of proteinaceous organic matter. This acid insoluble organic fraction of shell is primarily in the form of glycoproteins (Lowenstam and Weiner, 1989) whose isotopic and organic chemical composition at the molecular level arguably represents far more diverse paleo-proxy potential, but to date is less developed. Stable isotope proxies from carbon ($\delta^{13}C$) and nitrogen ($\delta^{15}N$) measured in shell matrix organic matter (OM) of ancient bivalves have the potential to record detailed ecological information for reconstructing past trophic and climatic conditions of nearshore environments. This is because, first, bivalve isotope values directly reflect local planktonic nutrient sources, abundance, and ecosystem structure, and second because sessile filter-feeding bivalves are passive recorders of water column organic matter sources at exactly known locations, thus integrating key isotopic signals into their tissues (Lorrain et al., 2002; Vokhshoori and McCarthy, 2014, Vokhshoori et al., 2014), including the biomineral fraction (e.g., Naito et al., 2010, 2013; Ellis and Herbert, 2014; Bassett and Andrus, 2021; Das et al., 2021; Graniero et al., 2016, 2021; Vokhshoori et al., 2022).

A major potential issue with shell matrix OM isotope records, however, is diagenetic alteration. Shell is a relatively porous matrix (Sykes et al., 1995), and so post-depositional conditions can expose shells to both physical and chemical weathering in which both contamination and post depositional alteration occur (Sykes et al., 1995). This can result in partial hydrolysis of the shell causing degradation of indigenous organic compounds either out of the shell matrix, or intrusion of exogenous compounds from the surrounding environment (e.g., humics derived from terrestrial C_3 or C_4 plants), altering the organic content composition and isotope values (Silfer et al., 1994; Sykes et al., 1995; Misarti et al., 2017). Finally, heterotrophic bacteria have also been shown to change the amino acid molar content of organic matter, and therefore can alter $\delta^{13}C$ and $\delta^{15}N$ signatures (Macko et al., 1987; Lehmann et al., 2002). While microbial alteration of shell OM has not been specifically investigated, similar effects are likely to occur. Overall, bulk $\delta^{15}N$ and especially $\delta^{13}C$ values have shown to change dramatically with increasing C/N ratios in degraded shell, often resulting in unreliable values (Ambrose, 1990; Ambrose and Norr, 1992; O'Donnell et al., 2003). However, an important limitation for understanding the potential of shell archives is that the exact mechanisms for change in bulk isotope values are typically unknown or not investigated.

In recent years compound-specific isotopes of amino acids (CSI-AA) of both carbon ($\delta^{13}C_{AA}$) and nitrogen ($\delta^{15}N_{AA}$), has emerged as a major tool to overcome multiple issues with traditional bulk isotope data. Whereas bulk isotope values inherently represent a mixture of the isotope signatures of all carbon and/or nitrogen containing compounds, CSI-AA measures only amino acids, the molecular constituents which make up proteins. This molecular specificity not only potentially avoids contamination issues with inorganic N or unknown N compounds, but also has now been shown to have enormous new information potential. By isolating a select group of molecules having known biochemical pathways and relatively predictable isotopic fractionation patterns with both trophic transfer and diagenesis (Ohkouchi et al., 2017), it is possible to directly compare AA isotope signatures of ancient shell with its modern analogue. CSI-AA is now increasingly used in ecological, biogeochemical and oceanographic studies for tracing food chain length (Choy et al., 2015; Loick-Wilde et al., 2019), reconstructing primary producer groups (Larsen et al., 2013; McMahon et al., 2015), and tracing inorganic nitrogen sources (Sherwood et al., 2014; Vokhshoori and McCarthy, 2014). However, while studies on bone have become relatively common (Ohkouchi and Takano, 2014), to date only a single study has directly examined CSI-AA signatures in archaeological invertebrate shell (Misarti et al., 2017). While these results suggested promise, there has never been a systematic examination of CSI-AA data or molecular change over a continuum of degradation states. If CSI-AA data can be applied in ancient shell samples, these molecular-isotope paleo-proxies would represent a major new tool to reconstruct local ocean biogeochemistry and primary production at both archaeological and potentially uplifted subfossil sites worldwide.

Here, we address for the first time the impacts of progressive diagenesis in the shell bound organic fraction on both bulk and compound specific isotope signatures by comparing the preservation isotope data for archaeological shell samples over a wide range of degradation states to their modern counterparts. We measured the elemental, molecular level, and stable isotope values of both $\delta^{13}C$ and $\delta^{15}N$ in bulk and CSI-AA within the shell matrix organic matter in mussels (*Mytilus californianus*) from modern and archaeological shells excavated from California's Northern Channel Islands ranging in age (6,100–250 cal BP) and depositional environments (e.g. exposed coastal bluff, buried strata, etc.), and evaluated these isotope data in the context of both molecular level AA composition of shell OM, and overall organic C/N ratios. We used this data to focus on two primary research questions: (1) can molecular and isotopic amino acid signatures help elucidate diagenetic mechanisms altering bulk isotope properties, and (2) how well are amino acid isotope proxies preserved in subfossil shells on multimillennial timescales? Answers to these questions will reveal the potential for CSI-AA to provide more accurate and diverse range of paleo-isotope information, which may transcend many of the known issues of bulk stable isotope values in degraded shell material.

2. Materials and methods

2.1. Sample collection, context, and processing

Data for modern *Mytilus californianus* shells was compiled from Vokhshoori et al. (2022). Modern shell from live, whole individuals of *M. californianus* were collected from Santa Cruz, CA (36°57′2 N, 122°2′39 W) between February 2018 to January 2019. Archaeological mussel shells were retrieved from the Santa Barbara Museum of Natural History collections. These museum specimens were excavated from midden sites around the Channel Islands and mainland Santa Barbara area; a summary of site chronology and context can be found in Table 1.

In the lab, bivalve shell samples were processed and prepared for elemental and isotope analysis similar to techniques performed by Misarti et al. (2017). For modern bivalves, soft tissue parts were discarded. Then all shells were scrubbed clean using a wired bristle brush and scalpel to remove periostracum and other large dirt particles. Shells were then soaked in a dilute 10% bleach (NaClO) solution for 1 hr, sonicated in nano-pure water, and dried in an oven overnight at 60 °C. Each shell was then crushed using a mortar and pestle and sieved through a 5 μm screen. For bulk $\delta^{15}N$ analysis, ~35 mg of non-acidified (i.e., non-demineralized) crushed whole shell was weighed into tin capsules. It is important to do bulk $\delta^{15}N$ analyses on non-acidified compounds, since acidification can alter or destroy N-containing compounds (Schlacher and Connolly, 2014), and can pose a risk of contamination from ambient gaseous ammonia released into laboratory air. In contrast, CSI-AA analysis cannot be impacted by inorganic N, or possible loss of non-AA compounds.

To extract the organic fraction, 1000 mg of sample was weighed into a labelled 20x150mm borosilicate vial and acidified with a weak 1 N HCl

Table 1
Sample Information.

Archaeological Site	Provenience	Location	Latitude	Longitude	Age (Cal BP)	Archaeological Context	Bulk Analyses (n)	CSI-AA Analyses (n)	Reference
–	–	Santa Cruz	36°57′2N	122°2′39 W	0	–	33	4	Vokhshoori et al. 2022
CA-SMI-470	Unit 2	San Miguel Island	34°4′15 N	120°24′55 W	460–250	Shell midden on marine terrace	10	2	Rick 2007
CA-SBA-4194	Level 3, 40–50 cm	Pt. Conception	34°26′25 N	120°28′10 W	900–220	Shell midden in coastal dune	10	3	Rick et al. 2022
CA-SBA-4187	Main midden, 50L	Pt. Conception	34°26′25 N	120°28′10 W	960–490	Shell midden in sea cliff	10	4	Rick et al. 2022
CA-SMI-481	East Dune	San Miguel Island	34°4′15 N	120°24′55 W	945–380	Shell midden in coastal dune	10	2	Rick 2007
CA-SMI-481	Unit 1, Level 3	San Miguel Island	34°4′15 N	120°24′55 W	1020–920	Shell midden in coastal dune	10	0	Rick 2007
CA-SMI-481	Unit 1b	San Miguel Island	34°4′15 N	120°24′55 W	1260–920	Shell midden in coastal dune	10	2	Rick 2007
CA-ANI-2	Unit 1/2	Anacapa Island	34°1′15 N	119°22′10 W	3250–2750	Shell midden on marine terrace	10	3	Rick and Reeder-Myers 2018
CA-SRI-191	Unit 1	Santa Rosa Island	33°58′24 N	119°57′57 W	6120–5840	Shell midden in coastal dune	10	4	Rick et al. 2006

by pipetting 1 mL increments until shell was completely dissolved (~35 mL); samples were stored in the fridge overnight to complete the reaction. After acidification, the organic fraction was isolated by filtration onto 22 mm 0.7 GF/F Whatman filters, rinsed thoroughly with nanopure water, and dried overnight at 60 °C. Sample yields were calculated based on total dry mass, ~0.5 mg was weighed into tin capsules for bulk $\delta^{13}C$ analysis, and the remaining amount was used for CSIA of AAs on a selected subset of shell samples.

2.2. NaOH clean tests

For a subset of shell samples (online data repository), we tested an additional NaOH cleaning protocol, targeted to remove potential contamination by intrusion of exogenous material, including plant matter and/or humic acids, proposed by Ambrose (1990). After complete demineralization and rinsing with nanopore water, each sample was submerged in ~ 35 mL of 0.125 M NaOH at room temperature for 20 to 24 h and then rinsed to neutrality with nano-pure water. Between rinses, samples were centrifuged at 3000 RPM for 5 min, the supernatant pipetted off and disposed of. Samples were lyophilized and yields were calculated.

2.3. Bulk Stable Isotope Analysis

Bulk stable isotopes of carbon ($\delta^{13}C_{bulk}$) and nitrogen ($\delta^{15}N_{bulk}$) were measured at the University of California Santa Cruz Stable Isotope Laboratory (UCSC-SIL) using a CE Instruments NC-2500 elemental analyzer coupled to a Thermo Scientific DELTAplus XP isotope ratio mass spectrometer via a Thermo-Scientific Conflo III. For high C content samples, automated in line CO_2 trapping is used to remove interference with N_2. Isotopes values are reported using delta (δ) notation: $\delta^{13}C$ or $\delta^{15}N = [(R_{sample}/R_{standard}) - 1] \times 1{,}000$, where R is the ratio of rare to common isotope of the sample (R_{sample}) and standard ($R_{standard}$), respectively, and corrected to VPDB (Vienna PeeDee Belemnite) for $\delta^{13}C$ and AIR for $\delta^{15}N$ against an in-house gelatin standard reference material (PUGel; ($\delta^{13}C = -12.6‰$, $\delta^{15}N = 5.6‰$) which is calibrated against international standard reference materials. Measurements are corrected for size effects, blank-mixing effects, and drift effects. An externally-calibrated Acetanilide standard reference material ($\delta^{13}C = -29.5‰$, $\delta^{15}N = 1.1‰$) purchased from Dr. Arndt Schimmelmann of Indiana State University is measured as a sample for independent quality control. Typical isotope ratio precision (1σ) is <0.1‰ VPDB for $\delta^{13}C$ and <0.2‰ AIR for $\delta^{15}N$.

2.4. Amino Acid Stable Isotope Analysis

Demineralized shell OM was analyzed for individual amino acid isotope values of both carbon and nitrogen following established McCarthy Lab protocols (e.g., McMahon et al., 2018). Briefly, ~3–5 mg of shell OM was weighed into 8 mL hydrolysis vials, submerged in 1 mL of 6 N HCl, purged with N_2 gas to remove oxygen, and hydrolyzed for 20 h at 110 °C. After hydrolysis, samples were cooled to room temperature and stored in a −4 °C freezer until further processing. After spiking samples with an internal standard Norleucine and drying hydrolysates at 60 °C under N_2, samples were then purified using cation-exchange chromatography with the DOWEX 50WX8-400 resin.

$\delta^{15}N$-AA and $\delta^{13}C$-AA values were measured as trifluoroacetyl isopropyl ester (TFA-IP) derivatives. Amino acid isopropyl esters were prepared with a 1:4 mixture of acetyl chloride:isopropanol at 110 °C for 60 min and then aceytlated using a 1:1 mixture of dichloromethane (DCM) and trifluoroacetic anhydride (TFAA) at 110 °C for 10 min (Silfer et al., 1991). Samples were again dried and finally re-dissolved in ethyl acetate for GC-IRMS analysis. AA isotopes values were measured using a Thermo Trace gas chromatograph coupled to a Finnegan Delta-Plus IRMS and GCC III (isoLink) at the UCSC-SIL. Using this method, we measured $\delta^{15}N$ and $\delta^{13}C$ values of the following AAs: alanine (Ala), glycine (Gly), threonine (Thr), serine (Ser), valine (Val), leucine (Leu), isoleucine (Ile), proline (Pro), aspartic acid (Asp), glutamic acid (Glu), phenylalanine (Phe), tyrosine (Tyr), and lysine (Lys). All sample derivatives were injected/quantified in triplicate. Measured $\delta^{13}C_{AA}$ values were corrected for the carbon atoms added during derivatization following the approach of Silfer et al. (1991) and Hare et al. (1991). Final isotope value accuracy and reproducibility was checked in two ways: first by comparison of the internal Norleucine standard with its known values, and second by assessing values of an in-house long-term McCarthy lab reference material (cyanobacteria), analyzed with every sample set according to McCarthy Lab protocols (Batista et al., 2014). Final $\delta^{13}C$-AA values were corrected for the added derivatizing reagents following the procedures of Silfer et al. (1991), and final $\delta^{15}N$-AA values were corrected based on the offset between known and measured $\delta^{15}N$-AA values of the calibration standard. Reproducibility, as estimated with standard deviation for samples, was on average less than <0.3‰ (range: 0.0–0.6‰) for carbon and <0.5‰ (range: 0.1–1.3‰) for nitrogen.

2.5. Amino-acid diagenetic parameters, ecological proxies, calculations and statistics

2.5.1. Amino acid diagenetic parameters

(1) Degradation Index (DI) – The DI is a widely used multivariate

approach for assessing the relative degradation state of organic material based on changes in relative amino acid composition (Dauwe et al., 1999). DI is defined as:

$$DI = \Sigma[var_i - Avg.\ var_i/SD\ var_i\ ] \times fac.coef \quad (1)$$

where var_i is the original (non-normalized) mole percentage of amino acid, Avg. var_i and SD var_i are the mean and standard deviation of modern shells in our dataset and fac.coef is the factor coefficient for amino acid *i* (Dauwe et al., 1999). DI is based on common proteinaceous AA composition of marine (plankton derived) organic matter however; and so the very different AA composition of shell structural protein, as well as possibly different lability, could potentially alter typical DI results. Therefore, while we use the standard DI formula (above), we use a slightly different interpretational framework, based on the known and constant AA composition of fresh shell OM: while only negative shifts in DI for mixed marine organic matter are interpreted as indicators of increased degradation, here we interpret any excursion from DI of modern shell (either positive or negative) as an indicator of diagenesis.

(2) CSI-AA biosynthetic patterns – In order to evaluate the preservation of AA isotope metabolic patterns, we normalized measured $\delta^{15}N_{AA}$ and $\delta^{13}C_{AA}$ values by subtraction from the average $\delta^{15}N$ (or $\delta^{13}C$) values of total hydrolysable amino acids (THAA):

$$\delta^{15}N_{AA\text{-}norm}\ (\text{or}\ \delta^{13}C_{AA\text{-}norm}) = \delta^{15}N_{AA} - \delta^{15}N\ THAA\ (\text{or}\ \delta^{13}C\ THAA) \quad (2)$$

where $\delta^{15}N_{THAA}$ (or $\delta^{13}C_{THAA}$) is the average of all measured AAs (Ala, Gly, Thr, Ser, Val, Leu, Ile, Pro, Asp, Glu, Phe, Tyr and Lys). This normalization approach allows direct assessment of biosynthetic signatures by removing any variability associated with changes in baseline changes between samples (e.g., time periods, sites).

(3) ΣV degradation parameter – An additional CSI-AA based degradation index, more specific to microbial alteration on amino acid isotope values, is the ΣV parameter, originally proposed by McCarthy et al. (2007), and now widely used to indicate specifically bacterial AA resynthesis (e.g., Shen et al., 2021; Vokhshoori et al., 2021). ΣV is a $\delta^{15}N_{AA}$-based proxy based on the average deviation of individual $\delta^{15}N$ values of trophic amino acids from the mean $\delta^{15}N$ value of trophic amino acids. We calculated ΣV values here using seven trophic amino acids (Glu, Asp, Ala, Val, Leu, Ile, and Pro):

$$\Sigma V = 1/n\Sigma Abs(\chi i) \quad (3)$$

where χ is the deviation of each trophic AA = $\delta^{15}N_{AA}$ − Avg. Trophic $\delta^{15}N$ (Glu, Asp, Ala, Val, Leu, Ile, and Pro), and n is the number of amino acids used in the calculation. Importantly, since AA isotope values are not linked to molar AA composition, $\sum V$ should not be impacted by the issues described above for DI.

2.5.2. Amino acid ecological proxies

Several CSI-AA-based ecological proxies were calculated as an additional check on the integrity of CSI-AA data based on well-known amino acid systematics.

(1) CSI-AA Baseline $\delta^{15}N$ – Nitrogen baseline isotope values from CSI-AA was estimated based on past work in molluscs (Vokhshoori and McCarthy, 2014). This parameter is from the non-fractionating source AA Phenylalanine.

$$\delta^{15}N_{Baseline} = \delta^{15}N_{Phe} \quad (4)$$

where $\delta^{15}N_{Phe}$ is the isotope value of Phenylalanine in a mollusc.

(2) CSI-AA Trophic Level – Because filter feeding mussels are primary consumers, they have essentially fixed trophic position near 2; any deviation from an expected range would indicate degradative shifts have occurred in either source or trophic AA groups respectively. We therefore used the recently published mollusc-specific TL equation developed using the same species in this study, *Mytilus californianus* ($TL_{CSIA\text{-}mollusc}$; Vokhshoori et al., 2022) which accounts for unique different trophic discrimination factors (TDF) specific to mollusc soft tissue, as well as an additional fractionation to shell matrix OM:

$$TL_{CSIA\text{-}mollusc} = 1 + [(\delta^{15}N_{Glu} - \delta^{15}N_{Phe} - \beta)/(TDF_{Glu\text{-}Phe} + \varepsilon_{shell})] \quad (5)$$

where $\delta^{15}N_{Glu}$ and $\delta^{15}N_{Phe}$ represent the stable nitrogen isotope values of bivalve Glu and Phe, respectively, β represents the difference in $\delta^{15}N$ between Glu and Phe of primary producers (3.4‰ for aquatic cyanobacteria and algae; McClelland and Montoya, 2002; Chikaraishi et al., 2009), $TDF_{Glu\text{-}Phe}$ 3.4‰, and ε_{shell} represents the observed fractionation (1.6‰) due to isotopic routing to the shell OM biomineral fraction.

(3) CSI-AA average $\delta^{13}C$ essential and nonessential AA – We looked at ecological parameters in carbon isotopes using the average $\delta^{13}C$ essential AAs ($\delta^{13}C_{EAA}$) and $\delta^{13}C$ nonessential AAs ($\delta^{13}C_{NAA}$). Animals must obtain EAAs from their diet, therefore $\delta^{13}C_{EAA}$ reflects dietary source (O'Brien et al.; 2002; Fogel & Tuross, 2003; Howland et al., 2003). In marine systems, the $\delta^{13}C_{EAA}$ is used to calculate primary production $\delta^{13}C$ value at the base of the food web (Vokhshoori et al., 2014; Shen et al., 2021; Vokhshoori et al., 2022). Nonessential AAs on the other hand can be synthesized *de novo* by animals and therefore the $\delta^{13}C_{NAA}$ reflects isotopic routing of a consumer's diet. $\delta^{13}C_{EAA}$ is the mol% adjusted measured average of six essential amino acids (Ile, Leu, Lys, Phe, Thr and Val), and $\delta^{13}C_{NAA}$ is the mol% adjusted measured average of six nonessential amino acids (Ala, Gly, Ser, Pro, Asx, Glx).

2.5.3. Bulk composition effects of contamination and diagenesis

(1) Exogenous contamination – For evaluation of elemental and isotopic shifts due to contamination from NaOH-base soluble components (e.g., humics, fulvics, C_3 terrestrial plant remnants, etc.), we measured the offset of bulk properties in shell samples that were cleaned with with 0.125 N NaOH (see Methods 2.2) and compared results with those from analogous untreated samples. We calculated offsets for the following variables: $\delta^{13}C$, $\delta^{15}N$, C/N ratio, wt% C and wt% N, and report differences as impacts of exogenous contamination.

(2) Diagenetic amino acid loss – We modeled the amount of isotopic change due to AA loss by calculating mol% weighted THAA values using molar compositions of modern vs. degraded shell. Specifically, we calculated the offset between mol% adjusted $\delta^{13}C_{THAA}$ (or $\delta^{15}N_{THAA}$) of modern shells (n = 4) using mol% distributions of modern shells, and then compared these results with those using the AA mol% distribution of our most degraded shell samples (C/N = 5.5–7.0). In other words, $\delta^{13}C_{THAA}$ (or $\delta^{15}N_{THAA}$) was calculated first using $\delta^{13}C_{AA}$ values and mol % values from modern shells. The same calculation was then used with the same modern $\delta^{13}C_{AA}$ values, but with "degraded" mol% values. The *difference* between these two values represents the change in THAA isotope value due to selected AA loss observed in degraded shell. Similarly, C/N ratio changes expected solely from AA loss observed were calculated using modern fresh shell AA molar distributions and the C/N ratio of each AA, and then molar distributions from our most degraded shell (C/N = 5.5–7.0).

2.5.4. Statistics

To test for differences between multiple groups we used a one-way ANOVA with Tukey's HSD test. We performed correlation matrix PCA; this allows comparison of variables with different units of measure. All analyses were performed in R (v.3.3.1) with RStudio interface (v.0.98.1028).

3. Results

3.1. Shell matrix OM yields

Sample yields were calculated as mass of shell fraction remaining after complete demineralization, recovered per gram of non-demineralized shell (Table S1). Modern sample yields were highest: for every gram of crushed shell, average OM yield was 7.9 ± 0.7 mg/g (range 6.7–9.3 mg/g; n = 28). Archaeological shell OM recovery was

lower and more variable. San Miguel Is. samples from all time periods had the highest average yields (4.0–5.6 mg/g) and lower yields from Anacapa (2.6 ± 1.1 mg/g), Santa Rosa (1.5 ± 0.7 mg/g) and Pt. Conception (2.4 ± 0.7 mg/g).

3.2. Elemental and bulk isotope values in shell matrix organic matter

Modern shell OM C/N ratios were low compared to archaeological shell from all time periods and islands. Mean C/N ratios for modern shell organics are consistent with pure protein, having C/N ratios of 3.0 ± 0.2, ranging from 2.8 to 3.5. Archaeological shell C/N ratios where universally higher, ranging from 3.4 to 9.5 and varied strongly across different island depositional locations. The Pt. Conception and Santa Rosa sites had the highest mean C/N ratios, 5.3 ± 1.4 and 5.1 ± 0.2, respectively, followed by Anacapa, with average values of 4.2 ± 0.3. Finally, shells from the San Miguel Island (Historic; Middle to Late Transition - MLT; and Late Periods) site had the lowest C/N ratios, 3.8 ± 0.3.

Bulk $\delta^{13}C$, weight %C (wt %C), bulk $\delta^{15}N$ and weight %N (wt %N) all showed consistent decreases with increasing C/N ratio (Tables S1 and S2, Fig. 1). For $\delta^{13}C$ values, regression of $\delta^{13}C$ vs. C/N was significant in archaeological shell ($P < 0.0001$, $R^2 = 0.63$) (Fig. 1a), while in contrast in modern shell $\delta^{13}C$ values showed no trend with C/N ($P = 0.41$, $R^2 = 0.0$) and the range of values were also narrow (−15.1 to −13.9‰). Within individual sites variability in $\delta^{13}C$ values was relatively narrow (2‰), except for Late Period San Miguel (−20 to −14‰) and Historic Pt. Conception (−22 to −15‰). Wt %C yield also displayed a significant negative correlation with C/N ($P < 0.0001$, $R^2 = 0.60$), while again within modern shell alone the regression was not significant ($P = 0.80$, $R^2 = 0.0$) (Fig. 1b). However, while $\delta^{13}C$ decreased linearly, the wt %C data show a more bimodal distribution (Fig. S1a), where one group centered around 40% wt %C and the second group around 10%.

Bulk $\delta^{15}N$ values also showed a significant negative trend with C/N ($P = 0.0001$, $R^2 = 0.13$), however far weaker than that observed for $\delta^{13}C$. In addition, $\delta^{15}N_{bulk}$ values a very weak but significant trend was observed in the modern group ($P = 0.03$, $R^2 = 0.15$) (Fig. 1c). Wt %N yield also showed a similar significant regression with C/N ratio as wt % C (Fig. 1d) ($P < 0.0001$; $R^2 = 0.71$), and a similar bimodal distribution, where most data centered around 14 wt %N, and a second smaller group of data clustered around 3 wt %N (Fig. S1b). Finally, the relationship between $\delta^{15}N_{bulk}$ values and wt %N yield was also significant ($P = 0.008$, $R^2 = 0.26$), with no significant trend for the same two variables when the modern group was analyzed independently ($P = 0.7$).

In addition to C/N ratio, weight %C and %N recoveries were also correlated with isotope values (Fig. S2). For both carbon and nitrogen, as wt %C or %N decreased, $\delta^{13}C_{bulk}$ values decreased ($R^2 = 0.78$, $P < 0.0001$), as did $\delta^{15}N_{bulk}$ values, however with far more variation and weaker regression ($R^2 = 0.26$, $P < 0.0001$). Overall, we found wt %C and wt %N yields both show a strong correlation with C/N ratio, in particular where C and N yields decreased to much lower concentrations below a C/N threshold of ~4 (Fig. 1). At the lowest end of wt % C and % N yields, stable isotope values also shift (Fig. S2). For carbon, shells with less than ~20% C show distinctly linear decreases in $\delta^{13}C$ values, while for nitrogen, as with almost all data described above, trends are far less clear.

A principle component analysis (PCA) synthesizes the main variables driving difference in the bulk dataset in statistical space (Fig. 2). We examined relations among five input variables: $\delta^{13}C$ values, $\delta^{15}N$ values, wt %C, wt %N and C/N ratios. PCA showed shell samples clustered mainly according to site (island). However, within this general pattern, some sites/islands were tightly clustered (Modern, San Miguel Is. Historic and MLT, Santa Rosa), while others showed far more scatter (Anacapa, Pt. Conception). A total of 93% of the variance was explained by the first two axes. The first principle component explained 79.8% of the variance and best separated the older shells (Anacapa and Santa Rosa) from the more recent time period shells, with the exception of shells from Pt. Conception (Historic Period). The second principle component explained 13.2% of the variance and separated Modern shells from San Miguel (Historic and Late Period). Wt %C and $\delta^{13}C$ variables directly overlapped, reflecting a strong covariance/correlation of the two variables. The near orthogonal angle between $\delta^{15}N_{bulk}$ with all the other variables, suggests that $\delta^{13}C$, wt %C and C/N are generally uncorrelated with $\delta^{15}N_{bulk}$ change, consistent with weaker regressions noted above. Moreover, parallel but opposing of wt %C and $\delta^{13}C_{bulk}$

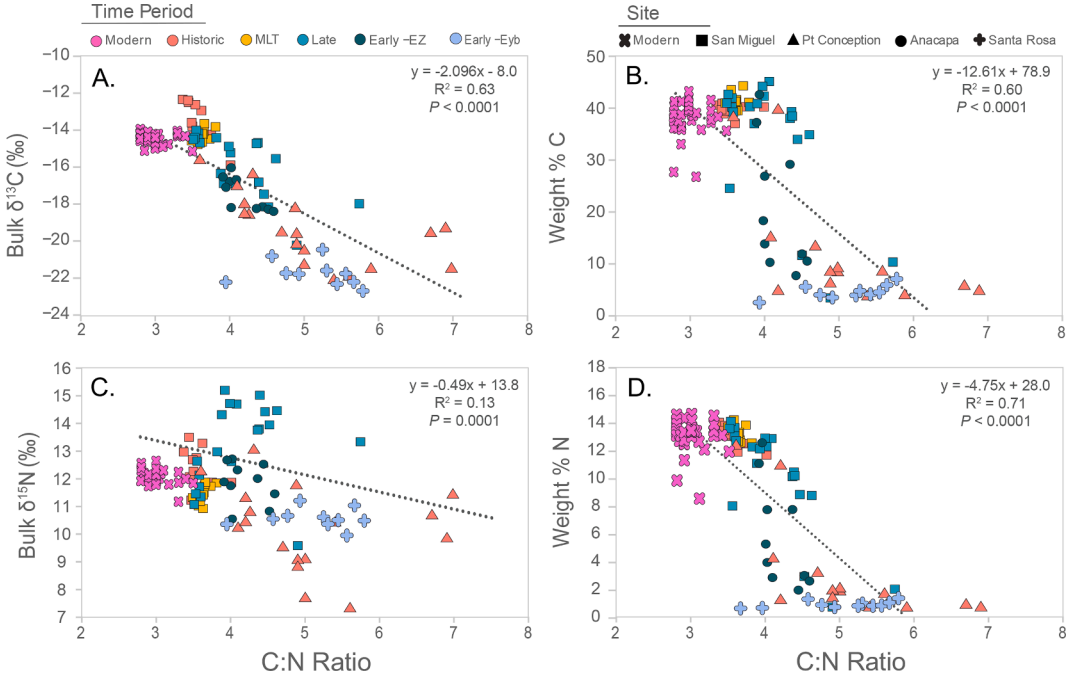

Fig. 1. Bulk isotope value trends with shell bound organic fraction C/N ratio organized by site (symbol shape) and time period (filled color; see legend on figure). Increasing organic fraction C/N ratios of individual mussel shells correlate strongly with (A) decreasing bulk $\delta^{13}C$, (B) decreasing weight %C yield, (C) decreasing bulk $\delta^{15}N$ and (D) decreasing weight %N yield.

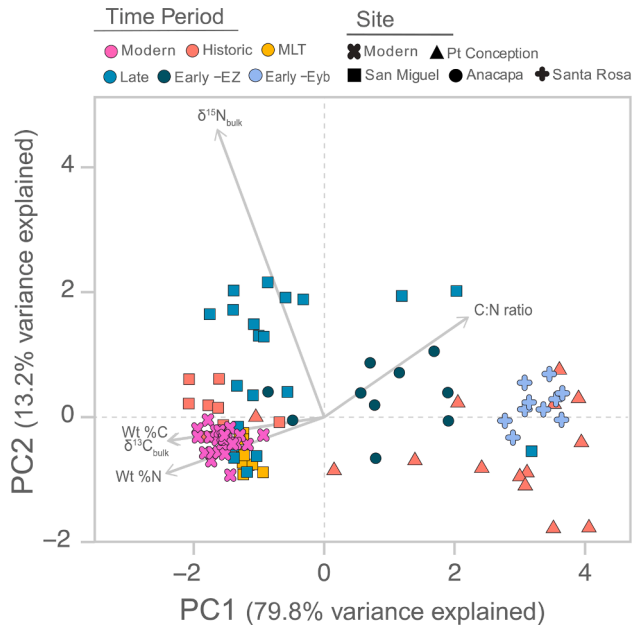

Fig. 2. Principle component analysis of bulk isotope and elemental results ($\delta^{13}C$, $\delta^{15}N$, weight %C, weight %N and C/N ratio) for modern and archaeological shells (see legend for time periods and sites). Vector length and direction represent relative loadings, indicating importance of each variable in separating each PC. The first principal component (PC1) explains ~80% of the variance and illustrates the strong inverse correspondence between C/N ratio and organic yields, $\delta^{13}C$. PC1 separates modern and San Miguel Is. from the other sites. The second principal component (PC2) explains about 13% of the variance driven by $\delta^{15}N$ values and separates Late Period San Miguel Is. from the rest of the sites.

vectors with C/N reflects a strong negative correlation.

3.3. NaOH cleaning tests

Results for the NaOH cleaning tests were plotted as the difference between treatment and non-treated fractions by subtraction of Post-NaOH from Pre-NaOH values for $\delta^{13}C_{bulk}$, wt %C, $\delta^{15}N_{bulk}$ and wt %N against C/N ratio (Fig. 3). In general, NaOH treatment showed "improvement", where improvement is defined as a shift in any values in ancient shell toward those which characterize shell matrix OM in modern shell (e.g., increased wt %C, or decreased C/N ratios). In most shells, C/N ratios decreased to below 4.0, wt %C, wt %N and $\delta^{13}C_{bulk}$ increased, while $\delta^{15}N_{bulk}$ values did not change. The magnitude of change depended on the shell's degradation state, as reflected by C/N ratios. Shells from the higher C/N group (e.g., 5.5–7.0) showed the greatest change from the base treatment, in which wt %C increased 20–40%, wt %N increased 0–15%, $\delta^{13}C_{bulk}$ values increased 3-6‰ and $\delta^{15}N_{bulk}$ values did not change; apart from one sample from Anacapa, the $\delta^{15}N$ value decreased by 8‰. Overall, regardless of the magnitude of change, nearly all base-treated archaeological shell elemental values shifted (or "improved") towards values considered typical of modern, fresh shell: wt %C 35–45%, wt %N 12–15% and C/N < 4 (Table S3).

3.4. Amino acid molar abundance distribution

Relative molar abundance data for modern and archaeological shells were grouped into four bins based on progressive increases in their C/N ratio bin (1) 2.5–3.3, bin (2) 3.4–4.3, bin (3) 4.4–5.4, bin (4) 5.5–7.0) (Fig. 4), as well as by site/location (Table S4). In all modern and archaeological shell, Ala and Gly dominated total AA composition (20–40 mol% each), followed by Ser and Asp (5–10 mol% each), irrespective of C/N ratio. Leu and Lys both made up ~ 5% in most samples, while other AA contributions were relatively minor (<5%). However, in contrast to modern shell where Gly mol% as most abundant followed by Ala, with increasing C/N ratios Ala mol% progressively increased compared to Gly mol%. Samples with highest C/N ratios (4.4–4.5 and 5.5–7.0 groups), were statistically distinct from modern shells (ANOVA, $F_{3,20} = 27.74$, $P < 0.0001$). Ser mol% was also different in all three groups compared to modern ($F_{3,20} = 11.15$, $P = 0.0001$). In Group 5.5–7.0 Pro mol% was different from modern (Tukey HSD *t*-test $P < 0.01$) and weakly different in Glu ($P < 0.05$) and Lys ($P < 0.05$).

Finally, we also more closely examined the molar abundance changes of the two most abundant amino acids, Gly and Ala across the dataset to understand how these mol% values shifted with increasing C/N ratio (Fig. 5). Since mol% data is inherently influenced by amounts of each AA recovered, we calculated Gly and Ala mol% abundance with and without Ala and Gly, respectively to look at possible mol% change independently from the other most abundant AA. Using all AAs in calculation, Mol% Gly (without Ala) steeply declines from values characteristic of modern shell when C/N ratios are higher than ~ 4.5 (Fig. 5a). In contrast, when Gly is not included in the calculation, the mol% Ala *increases* with increasing C/N initially, relative to modern shell values, then falls to levels similar or lower than modern values in shells with C/N ratios 5.5 or higher (Fig. 5b). The similarity of this result to that obtained using all AA (Fig. 4) shows that Gly changes do not drive these trends in mol% Ala. Finally, the ratio of Ala:Gly reflects these changes (Fig. 5c). Ala is lower than Gly in modern, fresh shell OM (Ala:Gly ~ 0.8) but increases in the archaeological shells (Ala:Gly 1.0–2.5).

3.5. Normalized amino acid carbon and nitrogen isotope values

Amino acid carbon and nitrogen isotope values were normalized to $\delta^{13}C_{THAA}$ and $\delta^{15}N_{THAA}$, respectively and plotted in terms of the C/N grouping defined above (Fig. 6). Measured non-normalized averages can be found in Tables S5 and S6. This normalization to THAA removes the influence of potential primary production baseline changes, allowing direct comparison of AA biosynthetic *patterns* between modern/unaltered shell and archaeological shell. In contrast to the bulk record, there were few differences in the carbon and nitrogen AA isotope patterns in archaeological shells across the C/N groupings examined. For $\delta^{13}C$ (Fig. 6a) two nonessential amino acids (NAA) had the largest differences ($\delta^{13}C_{Gly}$ and $\delta^{13}C_{Ser}$) with $\delta^{13}C$ values more negative for both AAs compared to modern shell. Specifically, the C/N 3.4–4.4 group $\delta^{13}C_{Gly}$ values were significantly lower by 8.2‰ (Tukey HSD *t*-test $P = 0.001$), in the C/N 4.5–5.4 range $\delta^{13}C_{Ser}$ was 6.0‰ lower and $\delta^{13}C_{Asp}$ 2.9‰ lower ($P = 0.04$ and $P = 0.02$), and in the C/N range 5.5–7.0 $\delta^{13}C_{Asp}$ was 2.5‰ lower ($P = 0.05$). In contrast, the essential amino acid (EAA) patterns were far more similar, however $\delta^{13}C_{Ile}$ was significantly 2.5‰ higher than modern in two C/N ranges (3.4–4.4 and 4.5–5.4; $P < 0.001$). There was also a weakly significant difference in $\delta^{13}C_{Lys}$ where values were 5‰ higher in the 4.4–5.4C/N group ($P = 0.02$) relative to modern.

$\delta^{15}N$ amino acid isotope patterns between modern and archeological shell also showed strong similarity (Fig. 6b). While not always statistically significant, two consistent differences were observed: $\delta^{15}N_{Asp}$ values were always lower in archaeological shell compared to modern (2.3–2.6‰) and $\delta^{15}N_{Ser}$ values were slightly higher (0.7–1.1‰) than modern. Statistically, C/N group 5.4–7.0 had significant differences in the most AAs compared to modern: $\delta^{15}N_{Thr}$ ($P = 0.01$), $\delta^{15}NS_{er}$ ($P = 0.02$) and $\delta^{15}N_{Asp}$ ($P = 0.02$). C/N group 3.4–4.4 also showed some differences, although weaker, for only two AA ($\delta^{15}N_{Thr}$, $P = 0.04$; $\delta^{15}N_{Val}$, $P = 0.02$). Notably, however, there were no significant differences in $\delta^{15}N_{Glu}$ and $\delta^{15}N_{Phe}$ between modern C/N and any other more degraded group; these two AAs that are commonly most used in ecological isotope proxies for reconstructing Trophic Level and $\delta^{15}N_{baseline}$ (Vokhshoori et al., 2022).

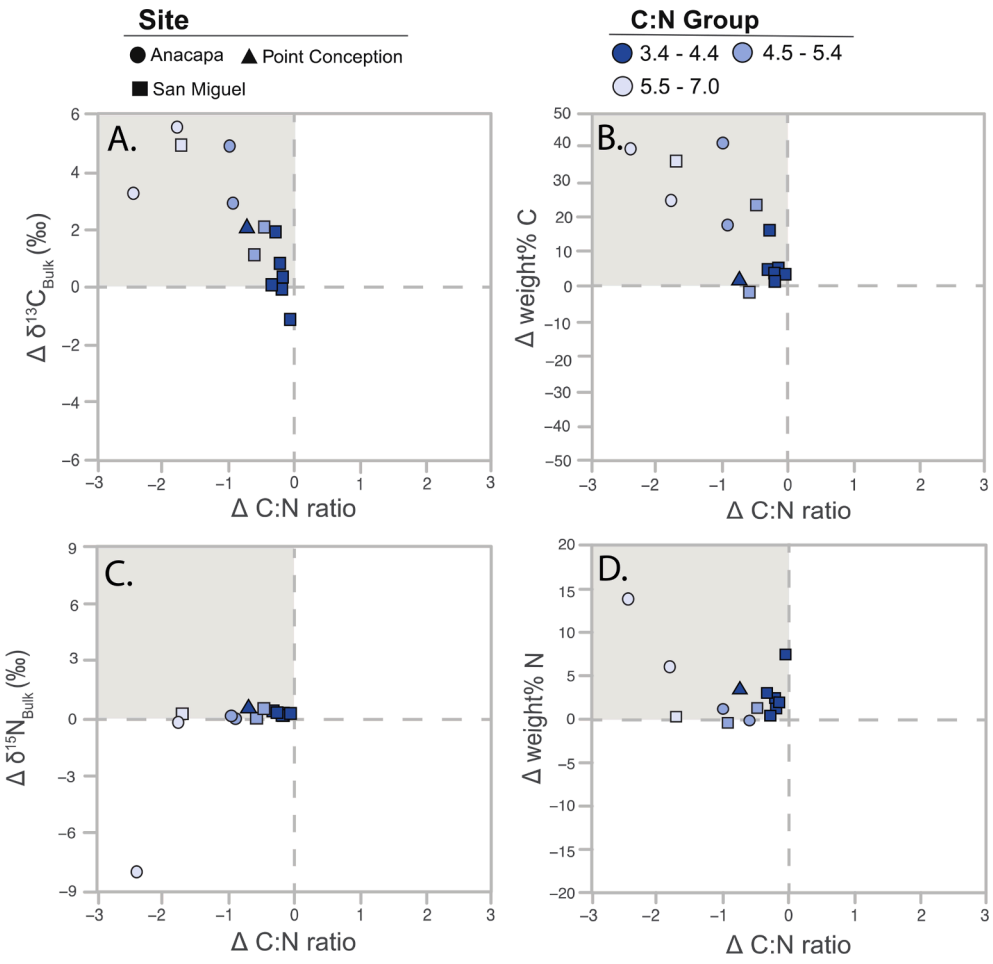

Fig. 3. Impact of base cleaning protocol on shell stable isotope values and organic yields. A 0.125 M NaOH cleaning process tested for impact of removal of potential contaminant compounds (e.g. lipids and humics; see Methods) in archaeological shell. Figures show the difference of post-treatment subtracted from pre-treatment for (A) bulk $\delta^{13}C$, (B) weight %C, (C) $\delta^{15}N_{bulk}$ and (D) weight %N plotted by difference in C/N ratio, organized by island (symbol shape) and C/N group (filled color); see legend on figure. Dotted lines indicate intersection of no change for reference and grey arrow indicates direction of "improvement," if any, defined as change toward values characteristic of modern shell OM values. Results indicate that most treatments appear to have removed some contaminants, shifting values toward those expected for modern shell.

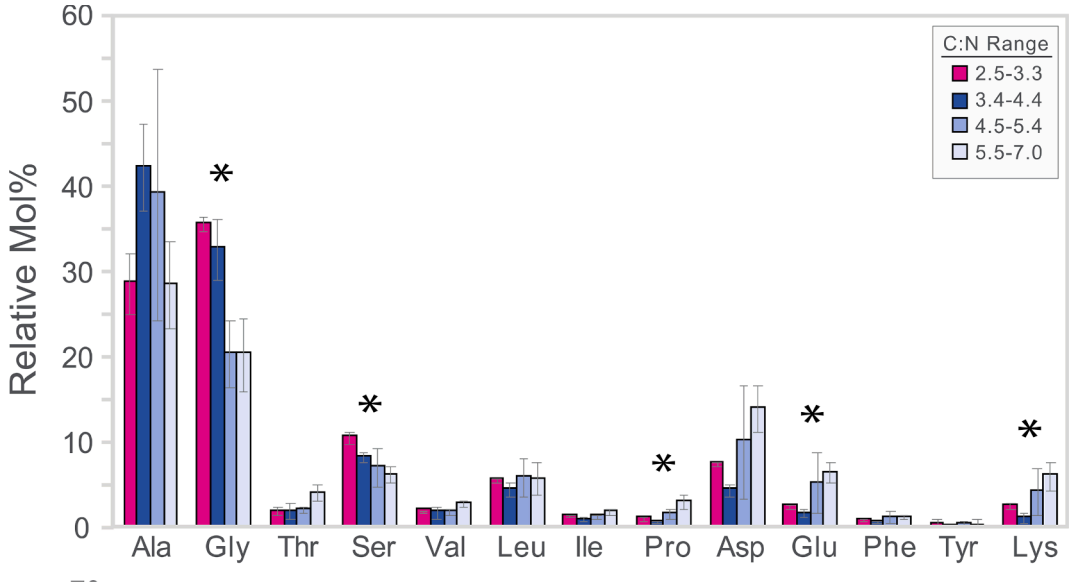

Fig. 4. Relative amino acid molar abundance ($Mol\%_{AA}$) organized by C/N group 2.5–3.4 (Modern; n = 4), 3.5–4.4 (n = 9), 4.5–5.4 (n = 6), 5.5–7.0 (n = 5) for all measured amino acids. Error bars indicate ±1 standard deviation of C/N groupings. AA for which more degraded C/N bins have significantly different isotope values from modern are indicated by *.

3.6. Amino acid diagenetic parameters and ecological proxies

We calculated several specific metrics for degradation and diagenesis from both AA molar composition changers, as well as CSI-AA data (see Methods 2.5). Multiple shell specimens had strongly altered DI values, however, this DI data did not fall out clearly as a function of relative

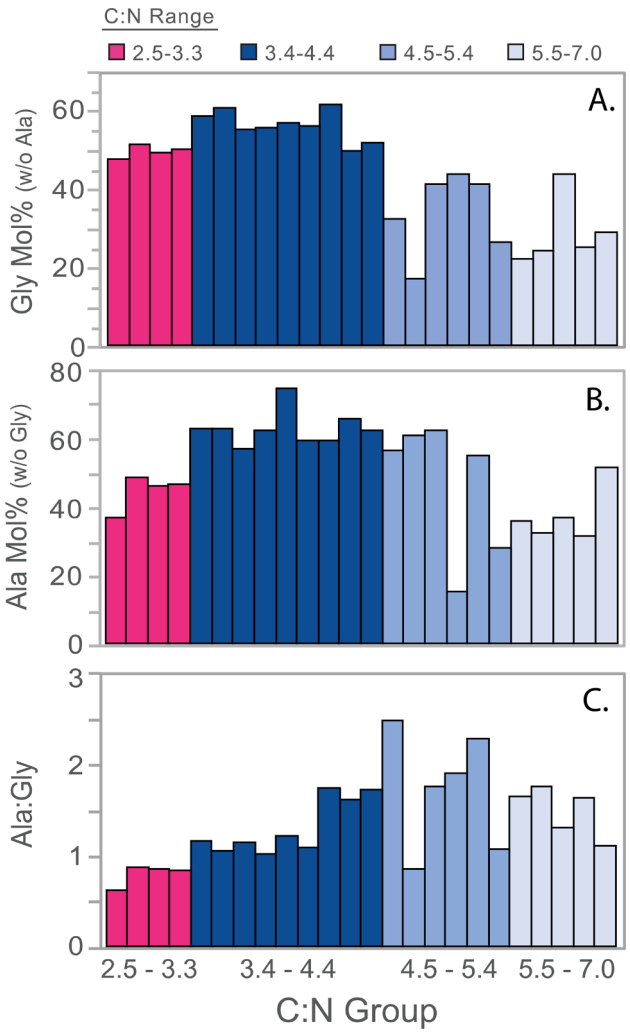

Fig. 5. Relative molar abundance changes of glycine and alanine to demonstrate change of each individual shell sample plotted by increasing C/N, color coded based on C/N group 2.5–3.4 (Modern; pink), 3.5–4.4 (dark blue), 4.5–5.4 (blue), 5.5–7.0 (light blue) for (A) glycine mol% (without alanine), (B) alanine mol% (without glycine), and (C) the ratio of alanine to glycine.

degradation, as expressed by increasing C/N ratios (Fig. 7a). Some elevated C/N samples had large positive excursions in DI, while others were negative. Overall, shifts in DI with increasing C/N ratio seemed to be location/site specific: Santa Rosa samples had the highest overall DI values (2 or greater), while in contrast, shells from Pt. Conception, while having the highest C/N ratios, showed no DI excursion away from modern values.

From $\delta^{15}N_{AA}$ data, we examined these parameters: ΣV, TL_{CSIA} and $\delta^{15}N_{baseline}$. For $\sum V$ (the microbial resynthesis index; eqn. (2), values of all archaeological shells fell close to the range of modern ΣV values (Fig. 7b), consistent with relatively unaltered δ^{15} $N_{AA\text{-}norm}$ patterns. Modern ΣV ranged between 1.2 and 1.6, while archaeological shells were on average 1.4 ± 0.3 (range from 0.9 to 1.9). $TL_{CSIA\text{-}mollusc}$ showed a similar tight range, with values also similar to those in modern shell (Fig. 7c): $TL_{CSIA\text{-}mollusc}$ of modern shells ranged between 1.8 and 2.0, while archaeological shells were on average 1.9 ± 0.2 and ranged from 1.6 to 2.3, excluding two outlying values that fell outside of the ±0.4 propagated error, one from Pt. Conception (1.5) and Late Period San Miguel (2.5). Finally, we plotted $\delta^{15}N_{Phe}$ values, our proxy for $\delta^{15}N_{baseline}$, and again found no statistically significant trend with C/N ratios ($P = 0.2$; Fig. 7d).

Finally, for $\delta^{13}C_{AA}$ we examined the relationship between mol% weighted NAA (Fig. 8a) and EAA (Fig. 8b) with increasing C/N ratio. In Mol% weighting, each AA isotope value is weighted to the percent abundance of that AA, and so this formulation can potentially better test if shifts on $\delta^{13}C_{bulk}$ values are driven by the isotopic composition changes within a given AA group (e.g., NAAs, EAAs or both). We found a significant decreasing trend in $\delta^{13}C_{NAA}$ values ($R^2 = 0.34$, $P = 0.0017$), but not in $\delta^{13}C_{EAA}$ values ($R^2 = 0.08$, $P = 0.184$) with C/N ratio.

3.7. Isotopic shifts linked to amino acid compositional change versus exogenous contamination

To estimate the magnitude of elemental composition and isotopic shift specifically due to mol% AA loss, we calculated C/N, and mol% weighted $\delta^{13}C_{THAA}$ and $\delta^{15}N_{THAA}$ from our CSI-AA data (see Methods 2.5.3). The expected C/N ratio of modern shell (calculated based on the average measured AA molar distribution in modern shell) was 3.3, which corresponded well with average C/N ratios of total bulk shell organic measured from EA-IRMS (3.0 ± 0.2, range: 2.8 to 3.5). Modeled C/N ratios based on AA molar composition measured in the most highly degraded shell was 3.7, indicating that ~0.4 increase in C/N ratio would be expected from the observed selective AA composition change. Modeled bulk isotopic shifts expected due to observed molar AA change in $\delta^{13}C_{THAA}$ and $\delta^{15}N_{THAA}$ values (a proxy for bulk isotopic shifts) yielded a 4.2 ± 0.5 *decrease* (range: −4.7 to −3.6; n = 4) in $\delta^{13}C_{THAA}$, but a negligible average 0.2 ± 0.2 *increase* in $\delta^{15}N_{THAA}$ values (range: −0.04 to 0.43; n = 4).

The relative magnitude of these isotope value changes from AA loss were then compared to isotopic change attributed to contamination by NaOH soluble organics (Fig. 9). While little to no change in $\delta^{15}N$ values could be attributed to either AA loss or contamination, for $\delta^{13}C$ values very large decrease in $\delta^{13}C$ values were observed for both mechanisms, with ~4‰ $\delta^{13}C$ decrease calculated for selected AA losses, and up to 5–6‰ *additional* $\delta^{13}C$ decrease (range: −1.0 to −5.5; n = 4) attributed to NaOH soluble contaminants. Cumulatively, for $\delta^{13}C_{bulk}$ the maximum net change suggested for both mechanisms combined is ~10‰, which is within the exact range in $\delta^{13}C$ value decreases we observed in our bulk isotope record (Fig. 1).

4. Discussion

Isotope proxies measured in fossil and subfossil archives is a common approach for reconstructing past environmental change, however, a precursor to using such archives is assessing the degree of diagenetic alteration at the geochemical level. This study investigates the elemental and molecular level changes in bulk and amino acid isotope patterns in the shell bound organic fraction of archaeological bivalve shells, across a range of ages and depositional environments. Strong diagenetic alteration to bulk isotope values in structural proteins such as bone and shell is well-documented (Ambrose and Norr, 1992; O'Donnell et al., 2003; Naito et al., 2010, 2013) and was also clear across our dataset (Fig. 1). Multiple mechanisms that have been proposed to drive such alteration, including physical processes, chemical reactions, and biological resynthesis (Mitterer, 1993; Macko et al., 1994), but without molecular level data it is typically not possible to distinguish between them. Understanding changes at a mechanistic level is critical for future applications of CSI-AA in archaeological and subfossil shell, since knowing not only extent of change, but also its main mechanism, is the key to understanding when isotope data from preserved archives remain viable. A main goal of this study was to test the idea that CSI-AA data that molecular level AA isotope measurements may also be able to overcome problems of diagenetic alteration in bulk isotope records for many degraded samples, while revealing underlying diagenetic mechanisms.

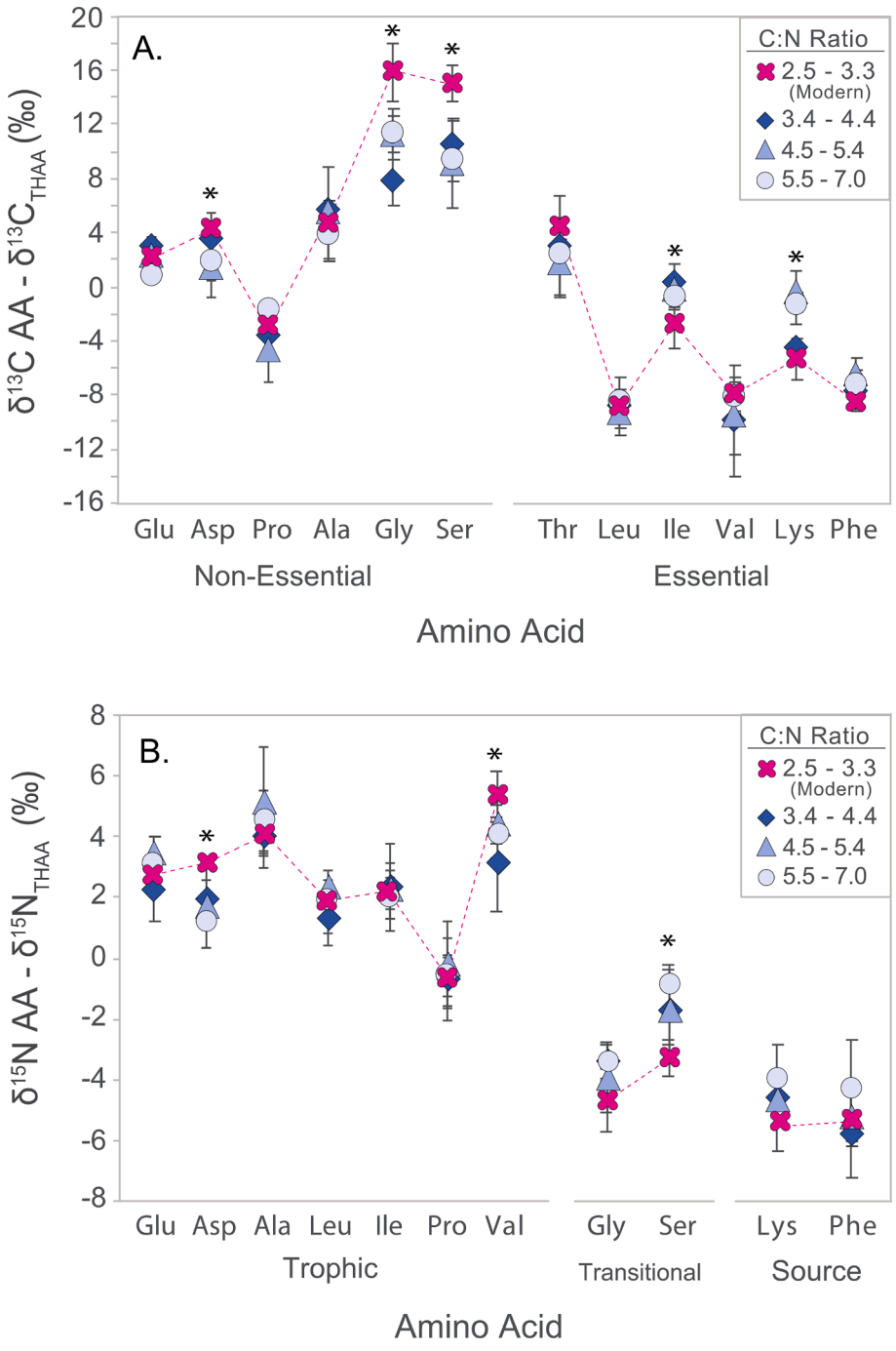

Fig. 6. Normalized (A) $\delta^{13}C_{AA}$ and (A) $\delta^{15}N_{AA}$ values in shell matrix OM of *Mytilus californianus* grouped by the C/N ratio. Normalization is by the subtraction of $\delta^{15}N_{THAA}$ or $\delta^{13}C_{THAA}$ (where the isotopic value of THAA is the average of Ala, Gly, Thr, Ser, Val, Leu, Ile, Pro, Asp, Glu, Phe, Lys (see methods). C/N groupings are as used in prior figures. Dotted line follows the mean value of modern shell. Error bars indicate ±1 standard deviation of C/N groupings. AA for which more degraded C/N bins have significantly different isotope values from modern are indicated by *.

4.1. Mechanism of diagenesis in archaeological shell matrix organic matter

4.1.1. Abiotic alteration vs. bacterial degradation

Shell matrix OM can undergo significant alteration over time due to physical processes, chemical reactions, and/or biological resynthesis (Mitterer, 1993; Macko et al., 1994; Sykes et al., 1995). Our archaeological shell samples underwent intensive diagenetic alteration as reflected in the large shifts observed in shell C/N ratios away from fresh modern shell values. Because C/N ratios in organic matter of unaltered shell are well constrained in a narrow range, we compare paleo-proxies and diagenetic parameters relative to C/N ratio changes, essentially treating this as a "master variable" to indicate relative degradation or diagenesis.

Shell matrix OM yields lower than modern (~8mg/1g shell), also clearly indicate removal of shell OM relative to inorganic components, however lower yields do not indicate if removal is physical or biological. The major physical processes affecting protein concentrations in shell are leaching and contamination, which have opposite effects on amino acid concentration and composition. While leaching decreases AA concentrations, contamination has the potential to increase them, but likely in a selective way. Fundamentally, however, leaching and contamination are caused by the same mechanism: water infiltrates the permeable pores of the shell and mobilizes indigenous organic compounds. This intruding aqueous phase not only can remove organic compounds from the shell matrix but can also introduce exogenous compounds from surrounding sediments or depositional environment (Sykes et al., 1995). The observation that our archaeological shells showed progressively

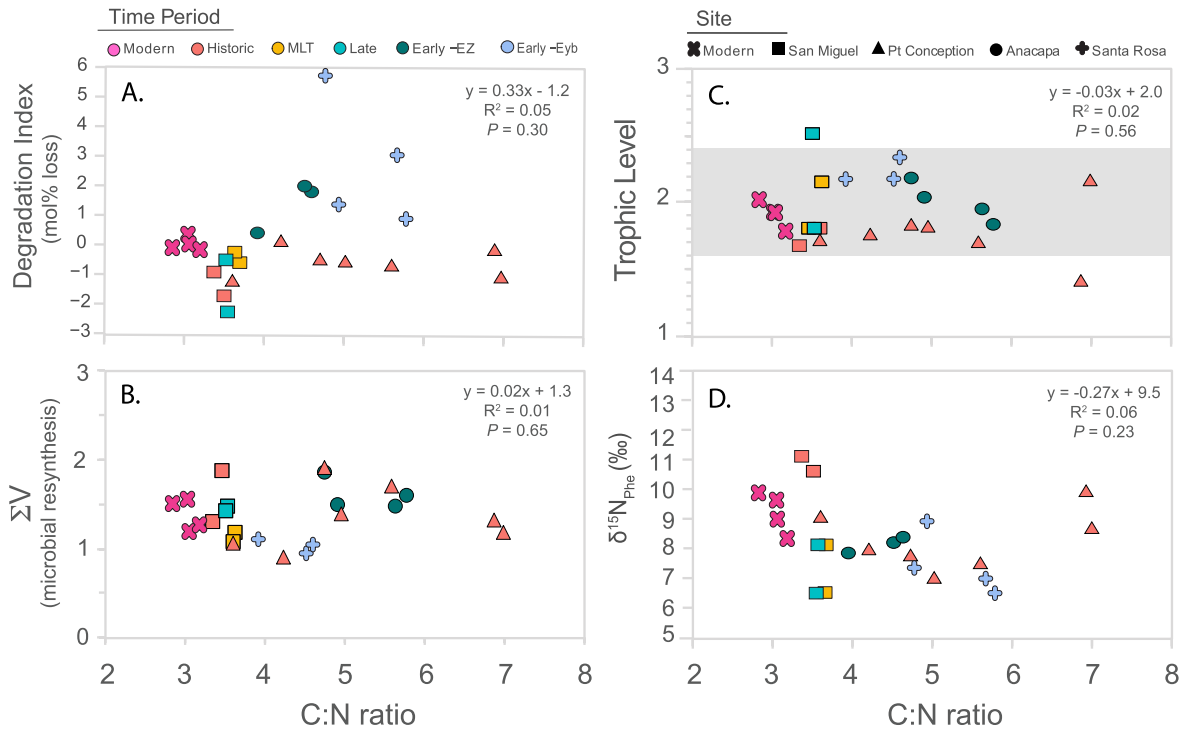

Fig. 7. Nitrogen and molar abundance parameters as additional checks for testing the preservation of isotope values versus C/N ratio grouped by site (symbols) and time period (filled colors). (A) Degradation index of amino acid molar abundance (eqn. (1)). (B) ∑V is the microbial synthesis index, values that hover between 1 and 2 suggest no alteration to the average $\delta^{15}N$ values of trophic AAs (eqn. (3)). (C) Trophic Level is a basic check on two key amino acids, Glu and Phe, used in the TL calculation, where the grey shading indicates ± 0.4 error propagated error in the calculation. TL estimations that fall outside of this range are altered in their $\delta^{15}N_{Glu}$ and/or $\delta^{15}N_{Phe}$ value (eqn. (4)). And (D) $\delta^{15}N_{Phe}$ our proxy for $\delta^{15}N_{baseline}$ values, also shows no trend with C/N indicating good preservation of this proxy (eqn. (5)).

decreasing OM yields with increasing C/N ratios strongly suggests that leaching was the dominant process for AA loss, although simultaneous contamination clearly occurred in some samples (Section 4.2).

Proxies for biological degradation further support the conclusion of yield loss primarily due to abiotic leaching. Specifically, the lack of any clear pattern in the DI parameter indicates no consistent alteration of AA mol% from microbial reworking. This is supported by the ∑V values in archaeological shell within the same range as modern shell (Fig. 7b). Importantly, while ∑V and DI are consistent, because ∑V is based on relative $\delta^{15}N_{AA}$ isotope patterns indicative of bacterial resynthesis (McCarthy et al., 2007; Calleja et al., 2013; Batista et al., 2014, Ohkouchi et al., 2017, and DI is based on AA molar abundance, they are fully independent. Finally, microbial reworking of organic matter typically *increases* Gly concentrations (Dauwe et al., 1999; Yamashita and Tanoue, 2003; Kaiser and Benner, 2009). In our data, the fact that Gly mol% *decreased* again supports the conclusion that decreased shell OM yields were not primarily due to microbial degradation.

4.1.2. *Bulk isotopic shifts linked to organic compositional change*

While physical removal, most likely from leaching, may explain the most loss of organic material (i.e., AA yield decreases, as well as decreases in weight %C and weight %N), it does not readily explain why $\delta^{13}C$ values dramatically decrease with C/N ratio increases, or the lesser changes in $\delta^{15}N$ values. For bulk isotope values and C/N ratios to change there must be either selective loss of certain AAs, addition of exogenous material with different isotope values, or loss of non-AA organic components.

Changes in relative composition of non-AA shell OM constituents represent one possibility for shifting both $\delta^{13}C$ and $\delta^{15}N$ values. Insoluble organic matter in calcitic and aragonitic shell is primarily composed of silk-like proteins rich in glycine and alanine. However, it also contains smaller percentages of saccharides in the form of chitin or its monomer glucosamine (Kobayashi and Samata, 2006; Marie et al., 2007; Agbaje et al., 2018) and a small amount of lipid (Farre and Dauphin, 2009). The matrix structure is thought to be an inner layer of chitin, bounded by silk-like insoluble proteins, to which are bound the acidic soluble matrix material (Weiner, 1983), having a physical structure somewhat like a sandwich (Risk et al., 1996). Because of the large differences in chitin vs. protein C/N ratios (~6 vs. ~3, respectively), protein loss alone could in principle alter bulk C/N ratios. However, given that saccharides make up <1% of the insoluble organic content (Agbaje et al., 2018), and their $\delta^{13}C$ values are not greatly different from bulk biomass (Hayes, 2001), this explanation seems unlikely for the large changes we observe. While there is little amino sugar $\delta^{15}N$ data, lower than expected $\delta^{15}N$ values for some amino sugars compared to bulk biomass (Macko et al., 1989) would at least suggest an *increase* $\delta^{15}N_{bulk}$ values with selected loss, in contrast to what we observe.

Lipids are also known to occur in shell and could shift bulk properties towards higher C/N ratios, and are also commonly ^{13}C-depleted compared to other biochemical classes (Hayes, 2001; DeNiro and Epstein, 1978; Tieszen et al., 1983). However, fresh shell OM C/N ratios suggest lipid content is likely very low (<10%,), suggesting that any lipid loss would be unlikely to have any significant impact on isotope ratios (Hoffman et al., 2015).

In contrast to these minor biomolecular components, alteration of protein AA composition in degraded shell is more likely to impact both $\delta^{13}C$ and $\delta^{15}N$ values and can be directly evaluated with CSI-AA data. As noted above, relative molar abundance of Gly decreased by 56% with increasing C/N, accompanied also by a clear decrease in Ala, and to a lesser extend Ser (Fig. 4). And for $\delta^{13}C$, the $\delta^{13}C_{AA\text{-}norm}$ values (Fig. 6) and mol% changes, strongly supports this as a main factor in bulk $\delta^{13}C$ change. In decreasing order mol% Gly, Ala, Ser and Asp are the four most abundant amino acids (Fig. 4); they also have the highest $\delta^{13}C$ values compared to all other AAs, where Gly and Ser $\delta^{13}C$ values are markedly higher than the rest (~12 – 20‰; Fig. 6). For $\delta^{13}C$ the largest calculated impact derived from $\delta^{13}C_{THAA}$ and mol% data (4.2‰ decrease

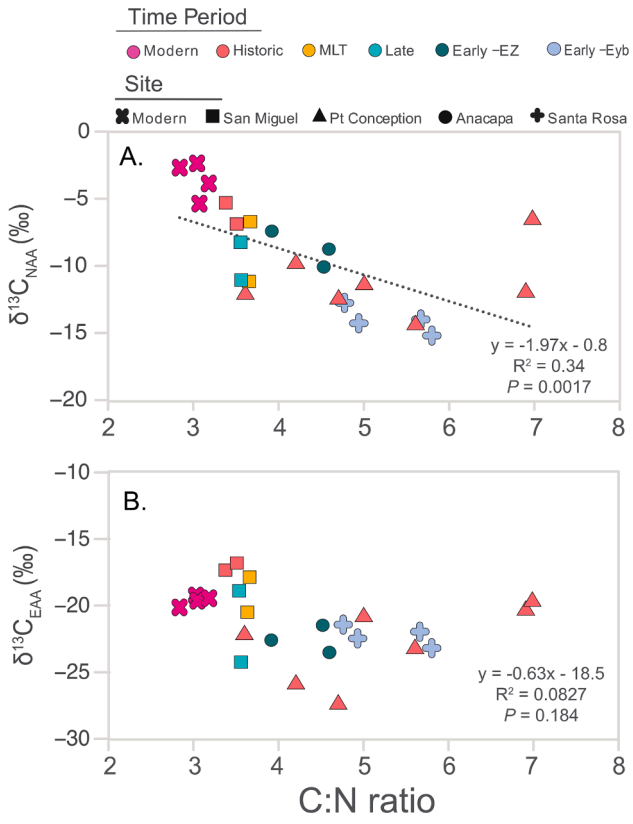

Fig. 8. Mean mol% adjusted (A) $\delta^{13}C$ of the nonessential amino acids (NAA; Ala, Gly, Ser, Asp, Pro and Glu) and (B) $\delta^{13}C$ of the essential amino acids (EAA, Thr, Val, Leu, Ile, Phe and Lys) versus C/N ratio grouped by site (symbols) and time period (filled colors) and the dotted line is the linear regression of the data, equation, R^2 and p-value noted on the figure.

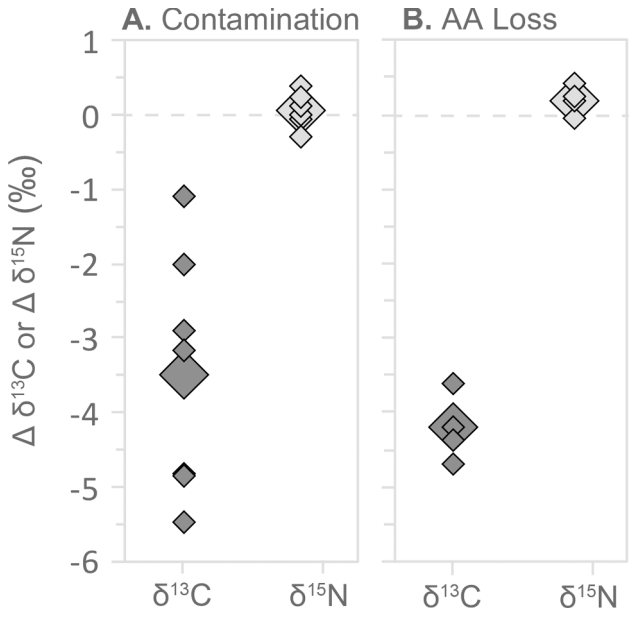

Fig. 9. Estimated carbon and nitrogen isotope effects from (A) contamination by NaOH soluble organics and (B) diagenetic loss of selected amino acids, primarily Gly and Ala. Isotope changes are calculated as difference between modern shell and samples with C/N > 4.5. Small diamonds indicate individual sample calculations and large diamond is the average. Stable isotope effects from removal of organic contamination and AA loss are calculated as described in the text (Methods, section 2.5.3).

for $\delta^{13}C$, Section 3.7) confirms that AA loss is a key factor in bulk $\delta^{13}C$ change. We note that the good agreement between our calculated modern shell C/N ratio (3.3) and measured C/N from EA-IRMS (3.0 ± 0.2, range: 2.8–3.5) also supports the validity of this approach.

However, the very different results for modeled $\delta^{15}N$ changes (0.2‰ increase for $\delta^{15}N$; Section 3.7) shows that mol_{AA}% shifts observed have very minimal impacts on bulk isotope values. This result overall indicates that the large molar losses of Gly and Ala appear to explain essentially none of the variation in $\delta^{15}N_{bulk}$. We hypothesize this could be linked to the fact that since proteins that undergo diagenetic alteration from deamination at the N-terminus, deamidation and hydrolysis does not change the $\delta^{15}N$ value of the peptide backbone (Ohkouchi and Takano, 2014). Whatever the mechanism, these observations implies if modern shell OM were to lose AAs in the same proportion as we observe in most degraded subfossil shells, it would result in major *decrease* in $\delta^{13}C_{bulk}$ values, and minimal impact in $\delta^{15}N_{bulk}$ values.

Finally, the strong decreases in only a few AA (mainly Gly, but also Ala) is opposite of those expected for proteinaceous bacterial degradation, where *increases* in both Gly and Ala Mol% have been suggested as microbial markers. This strongly suggests an abiotic mechanism. We hypothesize that dominant Gly loss resulted from abiotic aqueous Gly decarboxylation, a well-known reaction that cleaves the C-N bond via abiotic hydrolysis (Catão and López-Castillo, 2018), which has also been observed in subfossil deep-sea proteinaceous corals (Glynn et al., 2022). To our knowledge no Ala specific abiotic loss mechanism has been proposed, however the fact that Gly and Ala are the two smallest AA (smallest R group sidechains) at least suggests that molecular size/structure could be important analogous factors.

4.2. *Diagenesis or contamination?*

In addition to impacts of changes OM composition, because many shell mineral phases are intrinsically porous, exogenous contamination is a second major possibility for shifting bulk isotope values. Our weak base (NaOH) protocol (Ambrose, 1990) applied to a subset of shells should have been particularly effective at mobilizing C-rich compound groups (e.g., humic or fulvic acids) common in soil or fresh water.

Our results from NaOH cleaning strongly support the hypothesis that exogenous contamination in subfossil shells is a factor in shifting bulk parameters (Fig. 1). Our benchmark for "improvement" in each parameter (Fig. 3) was a change in values for base-cleaned organic isolates toward the values characteristic of modern shell isolates (shaded box in Fig. 3). For stable isotopes it is more problematic to define "improvement" in this way, especially for historical samples, because it is unknown what the isotope value should be in a given environment in the past without detailed background information. However, we nevertheless compared how isotope values shifted in relation to expected modern values (Fig. 3).

The overall observation that NaOH soluble materials affected all bulk parameters, and to a degree linked to degradation state, is consistent with assumed relative integrity of the inorganic matrix. As would be expected, NaOH cleaning produced only minor "improvement" for shells that were already near a modern C/N range (C/N group 3.4–4.4), and much greater "improvement" for shells that had C/N ratios higher than 4. While these data are generally consistent with past work (e.g., Ambrose 1990) supporting exogenous contamination from potentially organic and inorganic substances as exhibited by increased wt %C after treatment, shows it is important in bulk isotopic changes in archaeological samples. At the same time our data on molecular level change and mass balance isotope data strongly suggests that this is only one factor, and for many samples may be the minor one.

Taken together, our new data suggests the variation in the bulk isotope values is driven by two main mechanisms: exogenous contamination and diagenetic alteration in abundance of a few AA. Combining our isotope mass balance and NaOH cleaning data allows us to estimate the relative amount of change from each mechanism on bulk isotope

values of our shell samples. Specifically, we can evaluate changes from the same shell samples treated with and without NaOH base cleaning from contamination, and independently expected isotope shifts based on AA molar composition and CSI-AA signatures.

Fig. 9 shows the approximate impacts of presumed humic contamination (NaOH cleaning change) compared to those from AA loss. This comparison shows that humic contamination depleted $\delta^{13}C_{bulk}$ values as much as 5.5‰ (mean: 3.5‰ ± 1.6; n = 7) but had little to no effect on $\delta^{15}N$ values (mean: 0.1‰ ± 0.2; n = 6). Diagenetic loss of AAs (Section 4.1.2) in these shells caused decreases in $\delta^{13}C_{bulk}$ values up to −4.7‰ (mean: 4.2‰ ± 0.5; n = 4), but again does not appreciably impact $\delta^{15}N_{bulk}$ values (mean: 0.2‰ ± 0.2; n = 4).

4.2.1. What accounts for the large bulk $\delta^{15}N$ change in shell?

In contrast to $\delta^{13}C$ data, the large range in $\delta^{15}N_{bulk}$ values (6–7‰, Fig. 1) we observed with increasing C/N remain poorly constrained by either mechanism: neither AA molar loss nor removal of base-soluble contaminants in our experiments or calculations produce large $\delta^{15}N$ changes. The lack of change in $\delta^{15}N$ with NaOH cleaning (Fig. 3) is not surprising, since terrestrial humic materials typically have very low N content (e.g., de Leeuw and Largeau, 1993). The lack of significant $\delta^{15}N$ change due to selective AA loss is also very well constrained, due to directly measured mol% and $\delta^{15}N_{AA}$ values.

We hypothesize that large, site-specific shifts in $\delta^{15}N_{bulk}$ values may instead be the result of $\delta^{15}N$ baseline value (primary production $\delta^{15}N$) changes. Sediment cores from Santa Monica basin over the last 7,000 years have suggested similarly large baseline $\delta^{15}N$ value changes occur in this region over this time period (up to 7‰, Balestra et al., 2018). In addition, there is a very large and likely shifting spatial gradient in $\delta^{15}N$ values of primary production between the different Channel Island sites in the Santa Barbara Basin area, due to oceanographic and nutrient abundance changes from seasonal upwelling dominated northern CA margin, around point conception, and into year-round far less nutrient rich waters which characterize the S. CA bight (Checkley and Barth, 2009).

While deconstructing the relative influence of $\delta^{15}N$ baseline changes over time through in the Channel Islands is beyond the scope of this data set, the absence of clear influence of either base-removable contamination or diagenetic AA loss, coupled with clearly large and location-specific baseline variation in this region, suggests it as perhaps the most plausible hypothesis for $\delta^{15}N_{bulk}$ variation we observe. If this is correct, this in turn suggests that while bulk $\delta^{13}C$ values in degraded shell may be typically suspect and often highly altered, $\delta^{15}N$ values may be more reliable in many settings. However, this also likely would depend on clear and quantitative metrics for assessing shell OM alteration and degradation.

4.3. Is it possible to determine when shell bulk isotope values are reliable?

Our data clearly indicates several quantitative metrics which can now be used to address this key question of isotopic integrity in organics extracted from archaeological, subfossil or fossil mollusc shell specimen. First, C/N appears the simplest diagnostic indicator of preserved bulk isotope values, followed by weight %C and weight %N of the isolated organic fraction. As noted above, weak base cleaning can be important for determination of reliable bulk isotope values. We suggest that after NaOH cleaning protocols, C/N ratios together with wt% C and wt% N yields should all be assessed to evaluate likely quality of stable isotope data.

Overall, bulk isotope results indicate $\delta^{13}C$ and $\delta^{15}N$ values in bivalve shell can be reliably accepted in mussel shell with C:N ratios of <4.0, wt %C >30% and wt %N >10%. While modern mussel shells range from 2.8 to 3.5, it appears that minor degradation of shell OM content does not have a strong impact on either $\delta^{13}C$ or $\delta^{15}N$ isotope values. We suggest these bulk metrics must be applied to shells treated with NaOH base cleaning as well as untreated shell: while NaOH cleaning can shift some shell $\delta^{13}C_{bulk}$ values for samples with only minor or moderate degradation back toward to acceptable values, other shell might samples have undergone too much degradation to ever produce a reliable $\delta^{13}C_{bulk}$ value (Fig. 9).

4.4. Preservation of amino acid isotope values

In contrast to bulk data, the nearly identical overall CSI-AA patterns for both carbon and nitrogen between modern and all archaeological shells shows that key CSI-AA data appears to be largely unaffected by degradation over multi-millennial time scales, at least over the range of conditions represented by these samples (Fig. 6). This conclusion is based on THAA normalized CSI-AA patterns (Section 3.5) which indicate conserved patterns and therefore well-preserved individual AA values (Tuross et al., 1988; Vokhshoori et al., 2022), any substantial alteration in a single AA value would require that it no longer match the expected pattern, regardless of the normalization is applied. Overall, while a few AAs specific to either $\delta^{13}C_{AA}$ or $\delta^{15}N_{AA}$ data showed clear evidence of isotope fractionation with selective removal (discussed in next section) in general CSI-AA data was far better preserved than bulk isotope data, even in the most degraded samples.

4.4.1. $\delta^{15}N$ CSI-AA data

CSI-AA $\delta^{15}N$ parameters can further be used to assess preservation of key amino acid $\delta^{15}N$ values used in reconstructing certain ecological proxies (e.g., TL_{CSIA} and $\delta^{15}N_{baseline}$; Fig. 7c, d). Because the TL of any filter feeding mollusc is fixed at ~2.0, the TL_{CSIA} can be used to assess the fidelity of $\delta^{15}N$ values in two key AAs used in this calculation, Glu and Phe, calculated using a mollusc-specific TL equation (Vokhshoori et al., 2022). The observation that archaeological shell TL values fell within the error of modern TL estimations lends additional support to the conclusion from overall patterns that individual AA $\delta^{15}N$ values are well-preserved, at least for these AA. Further, the lack of correlation between $\delta^{15}N_{Phe}$ and C/N ratios is again consistent with TL_{CSIA} data, together indicating that $\delta^{15}N_{Phe}$ remains reliable for $\delta^{15}N_{baseline}$ reconstruction even over very wide diagenetic change in bulk C:N ratios.

Finally, despite the extremely large loss of Gly (Figs. 4 and 5), $\delta^{15}N_{Gly}$ values appear to not be altered at all within the $\delta^{15}N_{AA}$ pattern, even in the most degraded samples (Fig. 6). Since $\delta^{15}N_{Gly}$ also fractionates strongly with bacterial degradation (Calleja et al., 2013; Sauthoff, 2016), the observation of Gly removal without apparent Gly $\delta^{15}N$ fractionation further supports an abiotic loss mechanism.

4.4.2. $\delta^{13}C$ CSI-AA Data

The observation of $\delta^{13}C_{AA}$ pattern similarity (no statistical differences between EAAs in modern vs. archaeological shell; Fig. 6) indicates that individual AA $\delta^{13}C$ values are again well-preserved in all shells examined. However, in contrast with $\delta^{15}N$ data, the greater $\delta^{13}C$ variation observed in several NAAs (Gly, Ser and Asp) suggests that $\delta^{13}C$ fractionation is associated with AA having largest changes in $mol\%_{AA}$ abundances (Fig. 4). One important exception seems to be $\delta^{13}C_{Ala}$, which is the second most abundant AA in shell OM, and in contrast to Gly and other NAAs did not similarly fractionate with degradation (Figs. 5, 6).

While determining the exact mechanism for these $\delta^{13}C$ changes in only specific AA is beyond the scope of this paper, we note that preferential molar loss of abundant nonessential AAs (i.e., Gly and Ser) corresponded with $\delta^{13}C$ change. The direction of observed isotopic fractionation is consistent with abiotic hydrolysis of peptide bonds (Silfer et al., 1992, 1994), and/or the loss of specific functional moieties, and/or defunctionalization (Mitterer, 1993). As discussed above (Section 4.1), among the most likely mechanisms altering archaeological shell AA composition are physical leaching and abiotic chemical reactions. We hypothesize that such abiotic hydrolysis associated with physical leaching results in observed changes, consistent with the observations of a monotonic decreases in mol% of both these AA with

increasing C/N (Fig. 4a). Such $\delta^{13}C$ fractionation for these NAAs must alter the average $\delta^{13}C_{NAA}$ values in older shells, and in part likely contributes to significant trend decreasing with C/N ratio (Fig. 8A).

However, in contrast to these large $\delta^{13}C$ shifts observed in several NAAs, the consistency of the EAA data suggests that $\delta^{13}C$ CSI-AA proxies can still be reliably applied, even in very degraded shell. Most CSI-AA $\delta^{13}C$ proxies are based on essential AA, because this group best records baseline production $\delta^{13}C$ values (Shen et al., 2021; Vokhshoori et al., 2022), preserving "fingerprints" of primary producer types at the base of a food web (Larsen et al., 2013; Vokhshoori et al., 2014), and so can quantify the combination food resources of a consumer's diet (Stock and Semmens, 2016). The far greater consistency of $\delta^{13}C_{EAA}$ values (Fig. 6A) is also consistent with analogous work on progressive degradation of subfossil corals (Glynn et al., 2022), and is also reflected in the lack of any significant relationship between C/N and $\delta^{13}C_{EAA}$ (Fig. 8b). Overall, this data therefore suggests that in contrast to $\delta^{13}C_{NAA}$ values, in shell $\delta^{13}C_{EAA}$ signatures are far better well-preserved.

5. Summary and conclusions

This research is the first study to investigate the molecular level basis of bulk isotope diagenetic shifts in the organic fraction of mollusc shell. We examined changes in elemental and AA composition, and isotope signatures in the demineralized shell matrix organic matter of subfossil archaeological mollusc shells (*Mytilus californianus*), with a focus on preservation of compound-specific isotopes of amino acids, and how AA molar composition with progressive shell alteration changes in bulk elemental and isotopic properties.

Bulk stable isotope values are well-known to be affected by diagenesis, and our data illustrated this issue: very large changes observed in stable isotope values and shell organic matter yields, both strongly correlated with shifts in C/N ratio. Our data also indicated that above a shell organic threshold of 4 for C/N ratio, weight %C > 30% and weight %N > 10%, bulk isotope values remain accurate, and that incorporating an additional NaOH base cleaning step assist in reaching this threshold by removing C-rich contaminants, while not altering the isotope values of non-contaminated shells. Isotope mass balance calculation using CSI-AA data were also able to reveal the main mechanism of bulk changes, showing that selected AA loss during diagenesis accounted for about half of the largest $\delta^{13}C_{bulk}$ changes observed in the most degraded shell, but had little impact on $\delta^{15}N_{bulk}$ changes.

In contrast to very large bulk property shifts, CSI-AA data showed almost no alteration from expected patterns. $\delta^{13}C_{AA}$ and $\delta^{15}N_{AA}$ patterns, values, and CSI-AA paleo proxy reconstructions were all well-preserved, even in the most diagenetically altered shells. There were a few exceptions, however only for $\delta^{13}C_{AA}$ data. Specifically, $\delta^{13}C_{Gly}$ and $\delta^{13}C_{Ser}$ and $\delta^{13}C_{Asp}$ values showed evidence of isotopic depletion with progressive AA mol% removal, likely contributing to lower than average $\delta^{13}C_{bulk}$ values in more degraded shell. In contrast, for $\delta^{15}N_{AA}$ data no alteration of $\delta^{15}N$ values was observed for any AA, even for those such as Gly and Ala that showed very substantial molar losses. Overall, we conclude that even in the most diagenetically altered shell specimens examined here (~7000 Ybp, having highly elevated C:N > 7), key CSI-AA proxies for trophic level, baseline $\delta^{15}N$ and $\delta^{13}C$ values, and primary production fingerprinting applications could be reliably employed.

These new results demonstrate CSI-AA data as a novel approach to essentially "bypass" the very large impacts of diagenesis bulk isotope values in shell. CSI-AA analyses are becoming increasingly available, and coupled with rapid developments in CSI-AA ecological proxies (Ohkouchi et al., 2017) bivalve shell bioarchives can now be developed as entirely new realm in paleo-ecological and climatological research. These data will allow the examination of how past changes in climate affected nearshore ecosystem structure and biogeochemical cycling in specific to geographic regions. How far CSI-AA based information may be applied into the past from shell samples remains an open question. However, these data suggests that such data can be reliably obtained in a wide variety of archaeological samples spanning at least the early Holocene, across a wide range of depositional environments and preservation states. Importantly, the new data reported here also provides metrics which can be used to evaluate likely reliability of both bulk and CSI-AA data in very old or diagenetically altered samples.

Declaration of Competing Interest

The authors declare that they have no known competing financial interests or personal relationships that could have appeared to influence the work reported in this paper.

Acknowledgements

Fieldwork for this project was supported by Channel Islands National Park and The Nature Conservancy. We are thankful for the generosity of Santa Barbara Natural History Museum for supplying the archaeological shells in this study. We also thank the Santa Ynez Band of Chumash Indians Elders' Council for consultation related to this project. We thank Dyke Andreasen and Colin Carney (UCSC-SIL) for assisting with bulk isotopic analyses, and deeply grateful to Stephanie Christensen for assistance with CSI-AA analysis and always making sure the instruments were humming. This study was supported by National Science Foundation (BCS 2115154 and 2115145 to T.R. and M.D.M).

Appendix A. Supplementary material

Supplementary material of this manuscript includes data tables for bulk isotope and CSI-AA measurements (Tables S1–S6), more detailed interpretation of the bulk dataset (Figs. S1 and S2) and a map of SST of the southern California Channel Islands. Fig. S1 is a kernel density plot of weight %C and %N, and Fig. S2 is the relationship between weight %C (or %N) and $\delta^{13}C$ (or $\delta^{15}N$), respectively. Supplementary material to this article can be found online at https://doi.org/10.1016/j.gca.2023.05.005.

References

Agbaje, O.B.A., Ben, S.I., Zax, D.B., Schmidt, A., Jacob, D.E., 2018. Biomacromolecules within bivalve shells: Is chitin abundant? Acta Biomater. 80, 176–187.
Ambrose, S.H., 1990. Preparation and characterization of bone and tooth collagen for isotopic analysis. J. Archaeol. Sci. 17, 431–451.
Ambrose, S.H., Norr, L., 1992. On stable isotopic data and prehistoric subsistence in the Soconusco region. Curr. Anthropol. 33 (4), 401–404.
Andrus, C.F.T., 2011. Shell midden sclerochronology. Quat. Sci. Rev. 30, 2892–2905.
Balestra, B., Krupinski, N.B.Q., Erohina, T., Fessenden-Rahn, J., Rahn, T., Paytan, A., 2018. Bottom-water oxygenation and environmental change in Santa Monica Basin, Southern California during the last 23 kyr. Palaeogeogr. Palaeoclimatol. Palaeoecol. 490, 17–37.
Bassett, C.N., Andrus, F.T., 2021. Examining the potential of Pacific abalone as a novel high-resolution archive of upwelling in the California Current. Palaeogeogr. Palaeoclimatol. Palaeoecol. 571, 110342.
Batista, F.C., Ravelo, A.C., Crusius, J., Casso, M.A., McCarthy, M.D., 2014. Compound specific amino acid $\delta^{15}N$ in marine sediments: a new approach for studies of the marine nitrogen cycle. Geochim. Cosmochim. Acta 142, 553–569.
Calleja, M.L., Batista, F., Peacock, M., Kudela, R., McCarthy, M.D., 2013. Changes in compound specific delta N-15 amino acid signatures and D/L ratios in marine dissolved organic matter induced by heterotrophic bacterial reworking. Mar. Chem. 149, 32–44.
Catão, A.J.L., López-Castillo, A., 2018. On the degradation pathway of glyphosate and glycine. Environ. Sci. Processes Impacts 20 (8), 1148–1157.
Checkley, D.M., Barth, J.A., 2009. Patterns and processes in the California Current System. Prog. Oceanogr. 83, 49–64.
Chikaraishi, Y., Ogawa, N.O., Kashiyama, Y., Takano, Y., Suga, H., Tomitani, A., Miyashita, H., Kitazato, H., Ohkouchi, N., 2009. Elucidation of aquatic food-web structure based on compound-specific nitrogen isotopic composition of amino acids. Limnol. Oceanogr. Methods 7, 740–750.
Choy, C.A., Popp, B.N., Hannides, C., Drazen, J.C., 2015. Trophic structure and food resources of epipelagic and mesopelagic fishes in the North Pacific Subtropical Gyre ecosystem inferred from nitrogen isotopic compositions. Limnol. Oceanogr. 60, 1156–1171.
Das, S., Judd, E.J., Uveges, B.T., Ivany, L.C., Junium, C.K., 2021. Variation in $\delta^{15}N$ from shell-associated organic matter in bivalves: Implications for studies of modern and fossil ecosystems. Palaeogeogr. Palaeoclimatol. Palaeoecol. 562, 110076.

Dauwe, B., Middelburg, J.J., Herman, P.M.J., Heip, C.H.R., 1999. Linking diagenetic alteration of amino acids and bulk organic matter reactivity. Limnol. Oceanogr. 44, 1809–1814.
De Leeuw, J.W., Largeau, C., 1993. A review of macro- molecular organic compounds that comprise living organisms and their role in kerogen, coal, and petroleum formation. In: Engel, M.H., Macko, S.A. (Eds.), Organic Geochemistry, Principles and Applications. Plenum Press, New York, pp. 23–72.
DeNiro, M.J., Epstein, S., 1978. Influence of diet on the distribution of carbon isotopes in animals. Geochim. Cosmochim. Acta 42, 495–506.
Ellis, G.S., Herbert, G., 2014. Reconstructing carbon sources in a dynamic estuarine ecosystem using oyster amino acid $\delta^{13}C$ values from shell and tissue. J. Shellfish Res. 33, 217–225.
Farre, B., Dauphin, Y., 2009. Lipids from the nacreous and prismatic layers of two Pteriomorpha mollusc shells. Comp. Biochem. Physiol. Part B Biochem. Mol. Biol. 152, 103–109.
Fogel, M.L., Tuross, N., 2003. Extending the limits of paleodietary studies of humans with compound specific carbon isotope analysis of amino acids. J. Archaeol. Sci. 30, 535–545.
Glynn, D., Guilderson, T., McMahon, K., Sherwood, O., McCarthy, M.D., 2022. Investigating Preservation of Stable Isotope Ratios in Subfossil Deep-Sea Proteinaceous Coral Skeletons as Paleo-Recorders of Biogeochemical Information over Multimillennial Timescales. Geochim. Cosmochim. Acta 338, 264–277.
Graniero, L.E., Gillikin, D.P., Surge, D., Kelemen, Z., Bouillon, S., 2021. Assessing $\delta^{15}N$ values in the carbonate-bound organic matrix and periostracum of bivalve shells as environmental archives. Palaeogeogr. Palaeoclimatol. Palaeoecol. 564, 110108.
Graniero, L.E., Grossman, E.L., O'Dea, A., 2016. Stable isotopes in bivalves as indicators of nutrient source in the Bocas del Toro Archipelago, Panama. Peerj 4, e2278.
Hare, E.P., Fogel, M.L., Stafford, T.W., Mitchell, A.D., Hoering, T.C., 1991. The isotopic composition of carbon and nitrogen in individual amino acids isolated from modern and fossil proteins. J. Archaeol. Sci. 18, 277–292.
Hayes, J.M., 2001. Fractionation of carbon and hydrogen isotopes in biosynthetic processes. Rev Min Geochem 43, 225–277.
Hoffman, J.C., Sierszen, M.E., Cotter, A.M., 2015. Fish tissue lipid-C: N relationships for correcting $^{\delta 1}3C$ values and estimating lipid content in aquatic food-web studies. Rapid Commun. Mass Spectrom. 29, 2069–2077.
Howland, M.R., Corr, L.T., Young, S.M.M., Jones, V., Jim, S., Van Der Merwe, N.J., Mitchell, A.D., Evershed, R.P., 2003. Expression of the dietary isotope signal in the compound-specific $\delta^{13}C$ values of pig bone lipids and amino acids. Int. J. Osteoarchaeol. 13, 54–65.
Kaiser, K., Benner, R., 2009. Biochemical composition and size distribution of organic matter at the Pacific and Atlantic times-series stations. Mar. Chem. 113, 63–77.
Kobayashi, I., Samata, T., 2006. Bivalve shell structure and organic matrix. Mater. Sci. Eng. C 26, 692–698.
Larsen, T., Ventura, M., Andersen, N., O'Brien, D.M., Piatkowski, U., McCarthy, M.D., 2013. Tracing carbon sources through aquatic and terrestrial food webs using amino acid stable isotope fingerprinting. PLoS One 8, e73441.
Lehmann, M.F., Bernasconi, S.M., Barbieri, A., McKenzie, J.A., 2002. Preservation of organic matter and alteration of its carbon and nitrogen isotope composition during simulated and in situ early sedimentary diagenesis. Geochim. Cosmochim. Ac. 66 (20), 3573–3584.
Leng, M.J., Lewis, J.P., 2016. Oxygen isotopes in Molluscan shell: Applications in environmental archaeology. Environ. Archaeol. 21 (3), 295–306.
Loick-Wilde, N., Fernández-Urruzola, I., Eglite, E., Liskow, I., Nausch, M., Schulz-Bull, D., Wodarg, D., Wasmund, N., Mohrholz, V., 2019. Stratification, nitrogen fixation, and cyanobacterial bloom stage regulate the planktonic food web structure. Glob. Chang. Biol. 25, 794–810.
Lorrain, A., Paulet, Y.-M., Chauvaud, L., Savoye, N., Donval, A., 2002. Differential $\delta^{13}C$ and $\delta^{15}N$ signatures among scallop tissues: Implications for ecology and physiology. J. Exp. Mar. Biol. Ecol. 275, 47–61.
Lowenstam, H.A., Weiner, S., 1989. On Biomineralization. Oxford University Press, Oxford, p. 324.
Macko, A., Fogel, L., Hare, P.E., Hoering, T.C., 1987. Isotopic fractionation of nitrogen and carbon in the synthesis of amino acids by microorganisms. Chem. Geol. 65, 79–92.
Macko, S.A., Helleur, R., Hartley, G., Jackman, P., 1989. Diagenesis of organic matter - a study using stable isotopes of individual carbohydrates. Org. Geochem. 16, 1129–1137.
Macko, S.A., Engel, M.H., Qian, Y., 1994. Early diagenesis and organic matter preservation—A molecular stable carbon isotope perspective. Chem. Geol. 116, 365–379.
Marie, B., Luquet, G., Pais, De Barros, J.P., Guichard, N., Morel, S., Alcaraz, G., Bollache, L., Marin, F., 2007. The shell matrix of the freshwater mussel Unio pictorum (Paleoheterodonta, Unionoida). Involvement of acidic polysaccharides from glycoproteins in nacre mineralization. FEBS J. 274, 2933–2945.
McCarthy, M.D., Benner, R., Lee, C., Fogel, M.L., 2007. Amino acid nitrogen isotopic fractionation patterns as indicators of heterotrophy in plankton, particulate, and dissolved organic matter. Geochim. Cosmochim. Acta 71, 4727–4744.
McClatchie, S., Goericke, R., Leising, A., Auth, T.D., Bjorkstedt, E., Robertson, R.R., et al., 2016. State of the California Current 2015–16: Comparisons with the 1997–98 El Niño. California Cooperative Oceanic Fisheries Investigations Reports 57, 5–61.
McClelland, J.W., Montoya, J.P., 2002. Trophic relationships and the nitrogen isotopic composition of amino acids in plankton. Ecology 83, 2173–2180.
McMahon, K.W., Guilderson, T.P., Sherwood, O.A., Larsen, T., McCarthy, M.D., 2015c. Millennialscale plankton regime shifts in the subtropical North Pacific Ocean. Science 350, 1530–1533.
McMahon, K.W., Williams, B., Guilderson, T.P., Glynn, D.S., McCarthy, M.D., 2018. Calibrating amino acid $\delta^{13}C$ and $\delta^{15}N$ offsets between polyp and protein skeleton to develop proteinaceous deep-sea corals as paleoceanographic archives. Geochem. Cosmochim. Acta 220, 261–275.
Misarti, N., Gier, E., Finney, B., Barnes, K., McCarthy, M.D., 2017. Compound-specific amino acid $\delta^{15}N$ values in archaeological shells: Assessing diagenetic integrity and potential for isotopic baseline reconstruction. Rapid Commun. Mass. Spectrom. 31, 1881–1891.
Mitterer, R.M., 1993. The diagenesis of proteins and amino acids in fossil shells. In: Engel, M.H., Macko, S.A. (Eds.), Organic Geochemistry. Plenum Press, New York, pp. 739–753.
Naito, Y.I., Honch, N.V., Chikaraishi, Y., Ohkouchi, N., Yoneda, M., 2010b. Quantitative evaluation of marine protein contribution in ancient diets based on nitrogen isotope ratios of individual amino acids in bone collagen: an investigation at the Kitakogane Jomon site. Am. J. Phys. Anthropol. 143, 31–40.
Naito, Y.I., Chikaraishi, Y., Ohkouchi, N., Yoneda, M., 2013b. Evaluation of carnivory in inland Jomon hunter–gatherers based on nitrogen isotopic compositions of individual amino acids in bone collagen. J. Archaeol. Sci. 40, 2913–2923.
O'Brien, D.M., Fogel, M.L., Boggs, C.L., 2002. Renewable and nonrenewable resources: Amino acid turnover and allocation to reproduction in Lepidoptera. PNAS 99 (7), 4413–4418.
O'Donnell, T.H., Macko, S.A., Chou, J., Davis-Hartten, K.L., Wehmiller, J.F., 2003. Analysis of $\delta^{13}C$, $\delta^{15}N$, and $\delta^{34}S$ in organic matter from the biominerals of modern and fossil Mercenaria spp. Org. Geochem. 34, 165–183.
Ohkouchi, N., Takano, Y., 2014. Organic nitrogen: sources, fates, and chemistry. In: Falkowski, P.G., Freeman, K.H. (Eds.), Treatise on Geochemistry, second ed. Elsevier, Amsterdam, pp. 251–289.
Ohkouchi, N., Chikaraishi, Y., Close, H.G., Fry, B., Larsen, T., Madigan, D.J., McCarthy, M.D., McMahon, K.W., Nagata, T., Naito, Y.I., Ogawa, N.O., Popp, B.N., Steffan, S., Takano, Y., Tayasu, I., Wyatt, A.S.J., Yamaguchi, Y.T., Yokoyama, Y., 2017. Advances in the application of amino acid nitrogen isotopic analysis in ecological and biogeochemical studies. Org. Geochem. 113, 150–174.
Prendergast, A.L., Stevens, R.E., 2014. Molluscs (Isotopes): Analyses in Environmental Archaeology. In: Smith, C. (Ed.), Encyclopedia of Global Archaeology. Springer, New York, NY.
Rick, T.C., 2007. The archaeology and historical ecology of Late Holocene San Miguel Island. Cotsen Institute of Archaeology, University of California, Los Angeles.
Rick, T.C., Reeder-Myers, L.A., 2018. Deception Island: Archaeology of 'Anyapax, Anacapa Island, California. Smithsonian Contributions to Anthropology, Smithsonian Institution Scholarly Press, Washington, DC.
Rick, T.C., Robbins, J.A., Ferguson, K.M., 2006. Stable isotopes from marine shells, ancient environments, and human subsistence on Middle Holocene Santa Rosa Island, California, USA. J. Island Coast. Archaeol. 1, 233–254.
Rick, T.C., Braje, T.J., Graham, L., Easterday, K., Hofman, C.A., Holguin, B.E., Mychajliw, A.M., Reeder-Myers, L.A., Reynolds, M.D., 2022. Cultural Keystone Places and the Chumash Landscapes of Kumqaq', Point Conception, California. Am. Antiquity 1–18.
Risk, M.J., Sayer, B.G., Tevesz, M.J., Karr, C.D., 1996. Comparison of the organic matrix of fossil and recent bivalve shells. Lethaia 29, 197–202.
Sakuma, K.M., Field, J.C., Mantua, N.J., Ralston, S., Marinovic, B.B., Carrion, C.N., 2016. Anomalous epipelagic micronekton assemblage patterns in the neritic waters of the California Current in spring 2015 during a period of extreme ocean conditions. CCOFI Rep 57, 163–183.
Sauthoff, W., 2016. Nitrogen isotopes of amino acids in marine sediment: A burgeoning tool to assess organic matter quality and changes in supplied nitrate $\delta^{15}N$. University of California Press, Santa Cruz.
Schlacher, T.A., Connolly, R.M., 2014. Effects of acid treatment on carbon and nitrogen stable isotope ratios in ecological samples: a review and synthesis. Methods Ecol. Evol. 5, 541–550.
Shen, Y., Guilderson, T.P., Sherwood, O.A., Castro, C.G., Chavez, F.P., McCarthy, M.D., 2021. Amino Acid $\delta^{13}C$ and $\delta^{15}N$ Patterns from Sediment Trap Time Series and Deep-Sea Corals: Implications for Biogeochemical and Ecological Reconstructions in Paleoarchives". Geochim. Cosmochim. Acta 297, 288–307.
Sherwood, O.A., Guilderson, T.P., Batista, F.C., Schiff, J.T., McCarthy, M.D., 2014. Increasing sub-tropical North Pacific ocean nitrogen fixation since the Little Ice Age. Nature 505, 78–81.
Silfer, J.A., Engel, M.H., Macko, S.A., Jumeau, E.J., 1991. Stable carbon isotope analysis of amino acid enantiomers by conventional isotope ratio mass spectrometry and combined gas chromatography/isotope ratio mass spectrometry. Anal. Chem. 63, 370–374.
Silfer, J.A., Engel, M.H., Macko, S.A., 1992. Kinetic fractionation of stable carbon and nitrogen isotopes during peptide bond hydrolysis: experimental evidence and geochemical implications. Chem. Geol. 101, 211–221.
Silfer, J.A., Qian, Y., Macko, S.A., Engel, M.H., 1994. Stable carbon isotope compositions of individual amino acid enantiomers in mollusk shell by GC/C/IRMS. Org Geochem. 21 (6/7), 603–609.
Stock, B.C., Semmens, B.X., 2016. MixSIAR GUI User Manual.
Sykes, G.A., Collins, M.J., Walton, D.I., 1995. The significance of a geochemically isolated intracrystalline organic fraction within biominerals. Org. Geochem. 23, 1059–1065.
Tieszen, L.L., Boutton, T.W., Tesdahl, K.G., Slade, N.A., 1983. Fractionation and turnover of stable carbon isotopes in animals tissues: implications for $\delta^{13}C$ analysis of diet. Oecologia 57, 32–37.
Tuross, N., Fogel, M.L., Hare, P.E., 1988. Variability in the preservation of the isotopic composition of collagen from fossil bone. Geochim. Cosmochim. Acta 52, 929–935.

Vokhshoori, N.L., McCarthy, M.D., 2014. Compound-specific $\delta^{15}N$ amino acid measurements in littoral mussels in the California upwelling ecosystem: a new approach to generating baseline $\delta^{15}N$ isoscapes for coastal ecosystems. PLoS One 9, e98087.

Vokhshoori, N.L., Larsen, T., McCarthy, M.D., 2014. Reconstructing $\delta^{13}C$ isoscapes of phytoplankton production in a coastal upwelling system with amino acid isotope values of littoral mussels. Mar. Ecol. Prog. Ser. 504, 59–72.

Vokhshoori, N.L., McCarthy, M.D., Close, H.G., Demopoulos, A.W.J., Prouty, N.G., 2021. New geochemical tools for investigating resource and energy functions at deep-sea cold seeps using amino acid δ15N in chemosymbiotic mussels (*Bathymodiolus childressi*). Geobiology 00, 1–17.

Vokhshoori, N.L., Tipple, B.T., Teague, L., Bailess, A., McCarthy, M.D., 2022. Calibrating bulk and amino acid $\delta^{13}C$ and $\delta^{15}N$ isotope ratios between bivalve soft tissue and shell for paleoecological reconstructions. Palaeogeogr. Palaeoclimatol. Palaeoecol. 595 (2022), 110979.

Weiner, S., 1983. Mollusk shell formation: isolation of two organic matrix proteins associated with calcite deposition in the bivalve *Mytilus californianus*. Biochemistry 22, 4139–4145.

Yamashita, Y., Tanoue, E., 2003. Chemical characterization of a protein like fluorophores in DOM in relation to aromatic amino acids. Mar. Chem. 82, 255–271.